Effects of Nodalization on Containment Analysis in a Loss of Coolant Accident Using GOTHIC

Wilfred James McNeil IV

Thesis submitted to the faculty of the Virginia Polytechnic Institute and State University
in partial fulfillment of the requirements for the degree of

Master of Science
In
Mechanical Engineering

Mark A. Pierson, Chair
Robert E. Masterson
Danesh K. Tafti

April 29, 2013
Blacksburg, Virginia

Keywords: GOTHIC, Nodalization, Loss of Coolant Accident, Containment Model

Effects of Nodalization on Containment Analysis in a Loss of Coolant Accident Using GOTHIC

Wilfred James McNeil IV

ABSTRACT

Existing containment models for a loss of coolant accident at many nuclear power plants were created in the 1970s using older computer technology and thermal hydraulic models which were available at that time. While conservative, these models may not present the detail necessary to identify conditions which may be used to produce additional design margin for the plant.

After exploring containment and critical flow modeling, the basis for the use of GOTHIC in this analysis was established. A GOTHIC model was then created to simulate the loss of coolant accident results shown in an Updated Final Safety Analysis Report analysis for the North Anna Power Station. This model was used to examine the effects of increased nodalization in a subcompartment on the existing containment model.

It is shown that adding multidimensional sub-nodes to areas of interest can provide valuable detail which was absent in the UFSAR model. Simulations are able to show the localized pressure spike around a LOCA pipe break that quickly dissipates, leaving significantly lower pressures in what was once an averaged, single, lumped-parameter node. This suggests that additional design margin may exist depending on where the pipe break is assumed to occur.

Acknowledgements

I would like to thank first and foremost Dr. Mark Pierson for recognizing my potential as an undergraduate student and helping to guide me through the graduate school process. He is a fantastic professor that sparked my interest in nuclear engineering through exceptional lectures, a personal relationship to the field, and out of the classroom activities. His help and support has been invaluable over the past few years.

I would also like to recognize Dr. Danesh Tafti and Dr. Robert Masterson for helping to guide my thesis efforts as committee members. I would like to thank Dr. Masterson as well for his comments in the revision of this thesis. Additionally, the faculty and staff of the mechanical engineering department at Virginia Tech have been fantastic in helping to guide my efforts through my undergraduate and graduate career. Among others, Dr. Linda Vick, Dr. Al Wicks, Dr. Clint Dancey, and Ms. Cathy Hill have provided exceptional support and guidance.

For making this thesis possible, I would like to thank the engineering staff at Dominion Power. They have been beyond supportive in providing information, guidance, and help in reviewing and developing my GOTHIC models. John Harrell, Dana Knee, John Lautzenheiser, and Todd Flowers, thank you. Also, thanks to Jerry Bischoff for helping to create this partnership.

My knowledge of GOTHIC originated at a training course that was offered by Numerical Applications Inc. The generous support in training matters and answering technical questions by Tom George, Larry Wiles, and Nate Carstens was invaluable to my efforts.

Finally, I could not have accomplished what I have without the love and support of my wonderful family and friends, who are too numerous to name individually. They have been there for me through trying times and numerous obstacles, and have always been eager to help with anything, big or small. Thank you all.

Table of Contents

List of Figures

List of Tables

Abbreviations

Avg - Average

EPRI – Electric Power Research Institute

GOTHIC – Generation Of Thermal-Hydraulic Information for Containments

ft – feet (length)

lbm – pound mass

LOCA – Loss Of Coolant Accident

NAI – Numerical Applications Inc.

psid – pounds (force) per square inch, differential (with respect to node 10, bulk containment)

psia – pounds (force) per square inch, absolute

UFSAR – Updated Final Safety Analysis Report

1 Introduction

A reactor containment structure is designed to inhibit the spread of radioactive fission products in the event of a Loss Of Coolant Accident (LOCA). With the intent of further isolating the fluid released due to a pipe break, the reactor containment building is usually divided into a number of compartments, with each sub-compartment containing a system or part of a system. The design factor of safety limits the pressures allowed within the containment structure in order to prevent failure of either the outer structure or the subcompartment walls.

When setting the operational limits of the reactor, one limiting factor is the maximum pressure levels produced during a LOCA. Therefore, accurate models of a loss of coolant accident scenario are critical to setting appropriate design margins for the safe operation of the plant. Current models were developed when the plant was initially designed in the 1970s, using computers and thermal-hydraulic models available at that time. Portions of those models were created using slide rules, while others used computers which were comparatively limited in processing ability and computer memory relative to those in existence today.

Existing models divide a compartment into a number of nodes, and then implement a lumped capacitance model to calculate the pressure at each node. Another important factor to consider is how these models deal with critical flow phenomena between the nodes of lumped capacitance models when critical flow was deemed to exist within a given flow path. New computer modeling software is able to recalculate critical flow parameters in increments of 10^{-10} seconds and below.

It is reasonable, then, to assume that the existing containment models were simplified to accommodate the technology that was available at the time they were created, thus limiting plant capabilities. By using current computer models, it is hypothesized that a more realistic model can be created that may provide a design margin which might allow for a power up-rate in the reactor core or relax other existing safety criteria.

In order to fully understand what is happening during a reactor accident, it is necessary to examine how containment buildings are modeled and what major factor will affect fluid flows within a loss of coolant accident. Once this is established, it is possible to gain a full understanding of the model created previously to analyze the effects of a loss of coolant accident in a steam generator subcompartment of a containment building at the North Anna Power Station.

This analysis will address creating a containment model in GOTHIC, an accepted thermal-hydraulic modeling code, to simulate a loss of coolant accident in a steam generator sub-compartment. The GOTHIC computer simulation is based upon a containment model that was designed for the North Anna Power Station, which is considered a representative model for a pressurized water reactor in the United States. Currently, North Anna is operated by Dominion Power. Once a model is created that accurately recreates Dominion's results, as given in the Updated Final Safety Analysis Report, it can then be modified to explore if the existing nodalization scheme is adequate to provide the necessary detail for all design considerations, and what the effect of changing the nodalization may be.

2 Literature Review

2.1 Containment Modeling

2.1.1 Containment Structure

Containment structures are the ultimate barrier between the reactor system and the environment. They serve to protect the surrounding environment and public from the effects of the reactor, in terms of normal radiation exposure and in case of an incident, but also to protect the reactor from being affected by environmental or external influences. Thus, containment structures are designed to withstand design-basis accidents, and are regularly inspected to ensure that they remain in good structural condition.

The normal function of a nuclear containment building is to maintain constant operating conditions. Containments must be leak tight with respect to the environment. They are maintained at sub-atmospheric pressure so that if a leak does develop during normal operation, the flow direction will be into containment, rather than out, to prevent the release of radioactive particles[1].

Containments are selectively overdesigned with respect to normal operating conditions so that they may withstand certain foreseen possible scenarios, known as design bases. These design bases include, but are not limited to tornados, earthquakes, flooding, missiles, loss of coolant accidents, hydrogen explosions, criticality accidents, and fires [2]. The likelihood and severity of a potential event is evaluated on a case-by-case basis due to differences in geographic locations and plant design. When normal operating conditions are exceeded, and depending on

the severity of the impacts, the event may be known as a design basis event or design basis accident.

Many types of design basis accidents lead to a loss of coolant accident. Therefore, a containment structure must be able to meet several criteria to withstand this phenomenon. The containment must withstand the maximum pressures and temperatures generated by the release of high-energy water/steam, both on the exterior of the structure, and on internal structures which may experience local pressure differentials. The containment structure must also be able to cope with jet impingement, vibrations, and hydrogen gas release (and the possible associated explosion hazard), all while remaining leak tight [3].

As existing reactors age, continuing research is being done into nuclear containments in order to better model and explain various conditions and aging concerns. Nuclear reactors are limited to an operational duration of no more than 40 years on an original operating license. Utilities may apply for an extension of their license for another 20 years as the original license nears expiration. The degradation of operational and safety components due to age is the primary concern of the US Nuclear Regulatory Commission in the issuance of license renewals to operating power plants as they near the end of their original operating licenses. Thus, containment systems require continuing maintenance and inspection to ensure that they continue to serve their intended purpose [4].

2.1.2 Modeling Loss of Coolant Accidents

One of the most devastating design basis accidents for a nuclear power plant is a loss of coolant accident. Generally for a large primary loop break, coolant water flows from a pipe rupture causing pressure to drop within the steam supply system, allowing hot, pressurized water to flash

to steam, and potentially allowing the reactor core to dry out and melt down. Aside from the obvious loss of equipment and components within the plant, the out-flux of water and steam creates a complex multi-phase problem to solve in the interest of safety. There are numerous safety systems (with backups) which will engage to preserve a safe condition in this case, but the ability to model this type of accident becomes a key component to maintaining a safety plan [5].

Due to the large volume of a nuclear containment building, lumped parameter modeling techniques are generally used. Lumped parameter modeling is a method by which a system is spatially divided into a number of nodes, and the variables for mathematical calculations are taken to be an average value that applies to an entire division. Thus, a spatial range of values may be simplified into a smaller group of scalar numbers [6].

Computationally, lumped parameter models carry an advantage in the amount of computer resources that they require. Due to the fact that they employ averages instead of calculating full flow fields as a computational fluid dynamics code would, these models are able to account for larger volumes with fewer computer resources. There are limitations, however, such as a limited ability to calculate some mixing, fluid jet, and stratification phenomena [7].

Advanced lumped parameter methods have been developed to incorporate higher degrees of complexity in these models. By referring to various critical flow models, stratified flow models, and other such fluid and heat transfer relationships, these computer codes are able to overcome some of their inherent limitations.

Loss of coolant accident modeling can be successfully performed by using one of these lumped parameter codes. Generally, it is not necessary to obtain a great amount of local detail in a containment model, so the representative average given by a lumped parameter model is

sufficient. However, this thesis will explore the effects of providing additional division within a given volume for the purpose of providing additional insight into the actual temperatures and pressures that are generated during a LOCA.

2.2 Critical Flow Modeling

Critical flow, or choked flow, is a fluid dynamics phenomenon which limits the velocity of the flow of a compressible fluid through an orifice. This parameter becomes important when modeling fluid flows throughout a loss of coolant accident. Many models have been developed to attempt to accurately predict the effects of critical flow on a system.

For a single-phase ideal gas, the velocity of a flow is contingent on a few factors, but is relatively easy to calculate. The upstream and downstream pressures and specific heat ratio are all used to calculate the Mach number, and from that, the velocity. Assuming a frictionless, adiabatic environment where superheated steam may be treated as an ideal gas, the Mach number is given by the equation:

$$\frac{p}{p_0} = \left\{\frac{1}{1 + [(k-1)/2]Ma^2}\right\}^{\frac{1}{k-1}}$$

Where p is the upstream pressure and p_0 is the downstream or stagnation pressure, k is the specific heat ratio, and Ma is the Mach number, which can be solved [8].

Compressible fluids are limited to travel no faster than the speed of sound, or Mach 1. Velocity can be solved from the Mach number equation:

$$Ma = \frac{V}{c}$$

Where V is the velocity of the fluid and c is the speed of sound in a given medium. Below Mach 1, a change in the ratio between the upstream and downstream pressures will affect the velocity. Once Mach 1 is reached, no information about pressure may be passed through the stream, and the velocity becomes constant at its maximum value [8].

For two-phase flows, calculating the critical flow parameters becomes significantly more complex. Two-phase critical flow models are classified using a combination of two binary criteria. The model may be either in thermodynamic equilibrium or not in thermodynamic equilibrium, and it may be either homogeneous or non-homogeneous [9].

The question of thermodynamic equilibrium encompasses thermal, dynamic, and chemical equilibrium. Thermal equilibrium indicates that both the liquid and gas phases have the same saturation conditions. Dynamic equilibrium (or mechanical equilibrium) necessitates that both phases be well-mixed and have the same velocity. Chemical equilibrium requires that the density of both phases remains constant throughout the expansion [10].

Homogeneity is determined by the interaction between the two phases. If the two phases are well mixed and may be treated as a single mixture, a homogeneous model may be used. If there is any stratification in the flow or separation of the phases, a non-homogeneous model is required.

The homogeneous equilibrium model represents the basic approach for the classification that it represents. This model assumes that the fluid is a homogeneous mixture and that both phases are

in thermodynamic equilibrium. These simplifying assumptions lead to a basic model where the physical parameters for each component phase can be combined into a single set of parameters that represent the mixture [11]. Due to the fact that the fluid phases are considered to be homogeneous, there is no slip (or velocity difference) within the flow, as in other models. This model also largely neglects the impact of pipe walls and other phenomena (heat sources, friction, etc.), as they would throw it out of thermodynamic equilibrium.

The Moody model is a widely accepted non-homogeneous equilibrium model. The simplifying assumption used by the Moody model is that the flow is in thermodynamic equilibrium, however it allows for slip between the two phases. While slip is allowed in this model, thermodynamic equilibrium indicates that there can be no sheer stress between the phases or with pipe walls, and that each phase has a uniform velocity. Moody relies on the conservation of energy in order to tie this model together [12]. This model received some of the widest distribution, and is considered by the US Nuclear Regulatory Commission to be the best approach for modeling critical flow from long channels ($L/D>>1$) [13].

Hans Fauske presents another non-homogeneous equilibrium model. Again, this model assumes that the flow is in thermodynamic equilibrium, but allows slip between the phases. The key difference between the model that Fauske presents and Moody's model is that Fauske relies on conservation of momentum instead of conservation of energy [14]. The Fauske model also calculates the slip ratio relationship between the phase velocities differently [15].

The next category of models is non-equilibrium, homogeneous models. These are also referred to as "frozen" because they do not vary in mixture composition through the flow length. This indicates that the inlet and outlet quality will be the same, as will the velocity. There can also be

no heat or mass transfer between the phases [10]. Some of these models also introduce a multiplier, which represents different system changes in different models, but allows the models to be better fit to empirical data [13]. Moody would later release model updates that also included an empirical multiplier [16].

Burnell in 1947, and later Zaloudek present frozen models which calculate critical flow rate as a function of pressure differential between the upstream and downstream pressures. Both models use approximately the same equation, the key difference being in how they treat the empirical multiplier [13, 17]. The Zaloudek model was used in the creation of models for the North Anna Power Station Updated Final Safety Analysis Report (UFSAR) [18].

An experimental model is presented by Starkman et al. in 1964 which is also frozen. The authors point out in this model that the frozen condition may not be as limiting as one may think, because it takes approximately 10^{-4} seconds to travel through the nozzle [19].

Non-homogeneous, non-equilibrium models represent the fourth and final group of critical flow models. These models do not make many of the ad-hoc assumptions of the models thus far discussed, and are thus considerably more complex.

The Henry-Fauske model attempts to utilize the stagnation conditions in order to correct for the non-equilibrium flow [9]. This accounts for differing phase velocities and the impacts of wall stress. It does, however, assume that polytrophic expansion has a minimal effect on critical flow [10]. This model also uses an empirical multiplier to adjust the model, which in this case is proportional to the difference in exit quality [20].

Another non-equilibrium, non-homogeneous model is that developed by Ransom and Trapp. This model attempts to solve for critical flow velocity using differential equations which are not sensitive to discretized time steps [21].

One of the most complete models in this category is the Richter model. It uses two mass and two momentum conservation equations and one mixture equation, in addition to various stages of two phase flow and wall sheer stresses to calculate the critical flow conditions [20].

Critical flow modeling is a very diverse specialty within the engineering field, with a variety of models which are difficult to compare because they all use different methods to achieve similar ends [9]. While results are generally presented using different formats, one common metric for gauging the effectiveness of models is to compare them to empirical data drawn from Marviken Critical Flow Tests. These tests were conducted in the late 1970s at the Marviken Power Station facility south-west of Stockholm, Sweden. Many major thermal-hydraulic codes are tested to see how their implementation of critical flow models compares to empirical data obtained by the Marviken tests [10].

2.3 Existing Model

2.3.1 GOTHIC

The Generation Of Thermal-Hydraulic Information for Containments (GOTHIC) computer code is a widely used and vetted tool for modeling nuclear containment. GOTHIC was developed by Numerical Applications Inc. (NAI) for the Electric Power Research Institute (EPRI). It has been shown to produce accurate computational results, including the creation of a full-containment

model, and has passed review by the U.S. Nuclear Regulatory Commission [22, 23]. GOTHIC is being used around the world for containment analysis in nuclear power plant projects [24, 25].

Put succinctly by Dominion Power,

> "GOTHIC solves the conservation equations for mass, momentum and energy for multi-component, multi-phase flow in lumped parameter and/or multi-dimensional geometries. The phase balance equations are coupled by mechanistic models for interface mass, energy and momentum transfer that cover the entire flow regime from bubbly flow to film/drop flow, as well as single phase flows. The interface models allow for the possibility of thermal non-equilibrium between phases and unequal phase velocities, including countercurrent flow. GOTHIC includes full treatment of the momentum transport terms in multidimensional models, with optional models for turbulent shear and turbulent mass and energy diffusion. Other phenomena include models for commonly available safety equipment, heat transfer to structures, hydrogen burn and isotope transport." [26]

GOTHIC employs a lumped parameter modeling approach, as previously discussed, with the ability to perform multidimensional modeling tasks on subdivided volumes. Multidimensional modeling is achieved by subdividing a volume to attain greater accuracy. A volume may be subdivided in any combination of the three spatial dimensions to create a grid pattern. GOTHIC will treat each of these subdivided volumes as a local lumped parameter model element. The importance of using multidimensional modeling for additional detail is highlighted by Wolfe, Holzbauer, and Schall [27].

A GOTHIC model consists of basic elements which can be constrained to accurately represent any physical entity. Rooms and walls are modeled as control volumes, which are connected by flow paths and/or thermal conductors. Boundary and initial conditions must be specified for all volumes. Additional components such as valves, doors, fans, pumps, nozzles, and heaters/coolers may be added as necessary. GOTHIC is able to use these features and their interconnectedness to calculate desired outputs for each lumped parameter volume [28].

Some key parameters which are employed in this analysis are discussed below, but are by no means the extent of all input possibilities.

2.3.1.1 Control Volumes

Control volumes are the basic building block for a GOTHIC model. Every model must have at least one control volume. A control volume is a lumped parameter node, for which is calculated a single value for each variable applicable. This is done without regard to the size of the volume, or to the spatial location of the variable; thus the value of temperature, for instance, will be the same at the front, back, top, or bottom of the volume. A volume can be subdivided to provide more detail when it becomes necessary to know the value of variables at spatially specific points.

To build a GOTHIC model, certain parameters must be specified for each volume, including the following [28]:

1. Volume

   The volume required is the total free volume which is occupied by a fluid. Blockages, which represent anything that takes up space in the volume (such as equipment) may be added later which will reduce the effective area for calculation purposes.

2. Elevation

   The elevation of the floor of a control volume gives GOTHIC a reference point for further physical characterization.

3. Height

   Height is specified to give the volume dimension. When the volume is divided by height, the cross-sectional area of the volume is determined.

4. Hydraulic Diameter

   The hydraulic diameter is given by the equation:

$$D_H = \frac{4V}{A_W}$$

   Where V is volume and A_W is the wetted area within the volume. Hydraulic diameter is a variable in many fluid dynamics calculations.

5. Subdivided Volumes

   Each volume can be subdivided in order to obtain more degrees of freedom, provide more mechanistic physics, and obtain more detail to local conditions. However, additional parameters must be specified for subdivided volumes.

   a. Volume: height, width, and length are used in additional calculations
   b. Grid lines: the location of subdivisions are specified by a grid in the x-, y-, and z-axis

c. Blockages/Openings: geometric features can be specified within the volume to account for changes in features and the introduction of equipment
d. Volume variations and Cell faces: porosity, hydraulic diameter, droplets, and loss coefficients may be specified for each subdivision
e. Slip: slip boundary conditions determine the relationship between the fluid in cells, specifically if it encounters friction from physical walls or not

2.3.1.2 Flow Paths

Flow paths are hydraulic connections between either control volumes or boundary conditions. All flow paths are drawn from Volume A to Volume/Boundary Condition B, making positive flow in the direction from A to B. It is important to note that GOTHIC always conserves mass, energy, and momentum for all flow calculations [29]. Flow paths must have the following parameters specified [28]:

1. End Elevation

   The elevation with respect to the bottom of the model space must be specified. This elevation marks the bottom of the flow path, and must be above or equal to the bottom of the connecting control volume.

2. End Height

   The end height is the overall width of a flow path. When added to the end elevation, it gives the elevation of the top of a flow path. A flow path must fit within the dimensions of the control volume to which it connects.

3. Flow Area

   The flow area is the cross-sectional area of a flow path.

4. Hydraulic Diameter

   The hydraulic diameter is calculated for internal flow as

$$D_H = \frac{4A}{P_W}$$

   Where A is the cross-sectional flow area and P_w is the wetted perimeter. This is used in a number of fluid flow calculations.

5. Inertia Length

   Inertia length is used to indicate the relative length of a flow path, to determine how much inertia the fluid may develop as it travels. Included in the inertia length is also a factor of the size of the receiving volume, since some inertia will be carried past the end of the flow path. Because many of the flow paths in the models used are very short, their inertia length was set to an assumed value of 5 ft., while the flow path connecting to bulk containment is slightly longer and has the ability to develop slightly more inertia, and so has been set to a value of 20 ft. This is in order to best approximate the UFSAR values.

6. Friction Length

   Like inertia length, friction length is used to determine the amount of friction applied by pipe walls that creates drag on the fluid. Again, because the flow paths between most nodes are very short, friction lengths were generally set to 1 foot, while the friction lengths that connect to bulk containment were set to 5 ft., again to approximate the UFSAR values.

7. Relative Roughness

   Relative roughness is used with friction length to calculate the amount of drag on the fluid, as well as any mixing effects. Because no values were expressed in the UFSAR, this model employed all values of 0.1 for roughness.

8. Loss Coefficient

   Loss coefficients are calculated to represent how much pressure is lost to pipe and nozzle characteristics. GOTHIC requires both forward and reverse loss coefficients for internal flow, which for this model were assumed to be the same. It also requires an exit loss coefficient that represents any nozzle or exit conditions. These values were all tabulated in the UFSAR Table 6.2-30 [1]. These coefficients are combined to give GOTHIC an overall pressure change using the equation

$$\Delta p = (k + k_{exit})\frac{\rho v^2}{2}$$

   Where k represents loss coefficients, ρ is the density of the fluid, and v is velocity of the fluid [29].

9. Critical Flow Model

   GOTHIC also allows for the selection of which critical flow model it uses. For this analysis, the Homogeneous Equilibrium Model (HEM) was selected for all flow paths. However, GOTHIC is capable of solving a 9-equation model for three-dimensional critical flow in the liquid, droplet, and vapor phases, accounting for mass, energy, and momentum [30].

2.3.1.3 Boundary Conditions

GOTHIC considers a model to be a closed system, but allows for the specification of boundary conditions. Boundary conditions represent any influence from the outside of the closed system. The model used in this analysis uses flow boundary conditions, which specifies a mass flow rate, and utilizes pressure to determine the density of the incoming fluid. Rather than specifying pressure, however, the model used here specifies enthalpy of the incoming fluid instead.

2.3.1.4 Components

Many types of components are offered by GOTHIC, to include valves, fans, doors, nozzles, and more. The model created for this analysis uses only one type of component, a quick-open valve to represent blowout panels, which are tripped at a particular pressure.

2.3.1.5 Control Variables

Control variables are a powerful tool built into GOTHIC. They can be used to create a forcing function, a trip sense variable, or to create a special output. By inputting an equation, components, and arguments for calculation, GOTHIC can monitor parameters and use them for various purposes.

2.3.1.6 Initial Conditions

The ability to specify initial conditions is important for any model, but especially in containment modeling. Nuclear containments are regulated to maintain specific temperatures and sub-atmospheric pressures. For this analysis, these values were obtained from the UFSAR.

2.3.1.7 Run Control

Run control is a particularly useful section of GOTHIC, which allows the user to specify the length of the transient, the maximum time step, and how GOTHIC will measure variables. Print and Graphics intervals are specified, which control how often the program will output values for analysis. Intervals that are too long will return values that pass over details in a calculation, while intervals that are too short are very computationally expensive. It is important to find the proper balance in these parameters.

2.3.1.8 Graphs

The primary output method for GOTHIC is graphs. The graphs menu is capable of building plots based on nearly any variable that is calculated by GOTHIC. If a custom output variable is desired, a control variable can be created to measure the custom output, and can be graphed. When a model is run more than once (due to changes, etc.), the graphs will not be updated until told to do so via the "replace graph data" button. Graphs can contain up to five plotted lines, and may be customized to best display the data.

2.3.2 North Anna Model

Since the North Anna nuclear power station was used as a reference for representative design data, the specifics of the North Anna containment structure need to be discussed. North Anna operates two Westinghouse 3-loop pressurized water reactors with single pressurizer each [31].

Each reactor has its own containment structure, which is a concrete dome reinforced with pre-stressed rebar [32]. The containment structure is compartmentalized in order to restrict the flow of material should a loss of coolant accident occur. As shown in Figure 1 and Figure 2, walls separate the different compartments, and the configuration of those walls changes depending on elevation. Between the compartments are vents and blowout panels. That way, if an accident does occur, fluid will build up in a particular compartment but will be vented to bulk containment in order to prevent failure of walls between compartments [1, 33].

Figure 3F-4 (SHEET 1 OF 4)
CONTAINMENT STRUCTURE

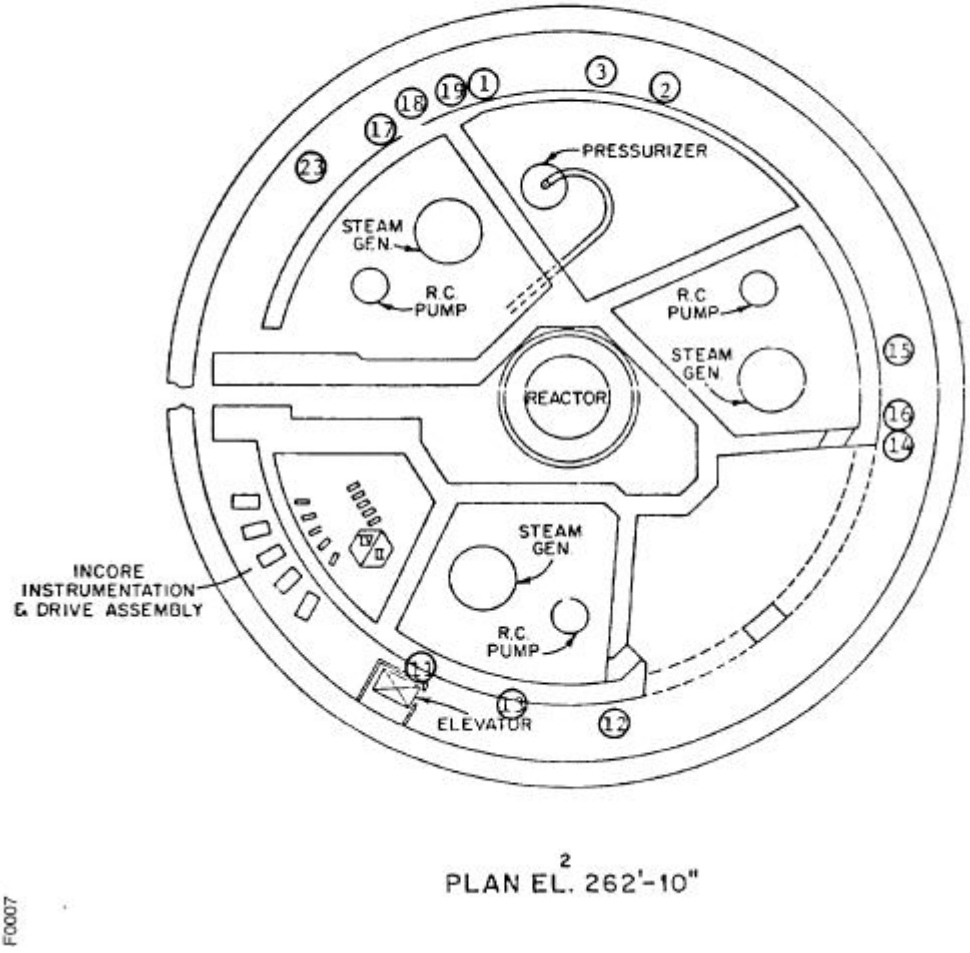

Figure 1: Cross-sectional top view of contianment structure from elevation 262'10", showing locations of walls, subcompartments, and major equipment [33]. Copyright Dominion Power; Used with permission.

Figure 3F-4 (SHEET 4 OF 4)
CONTAINMENT STRUCTURE

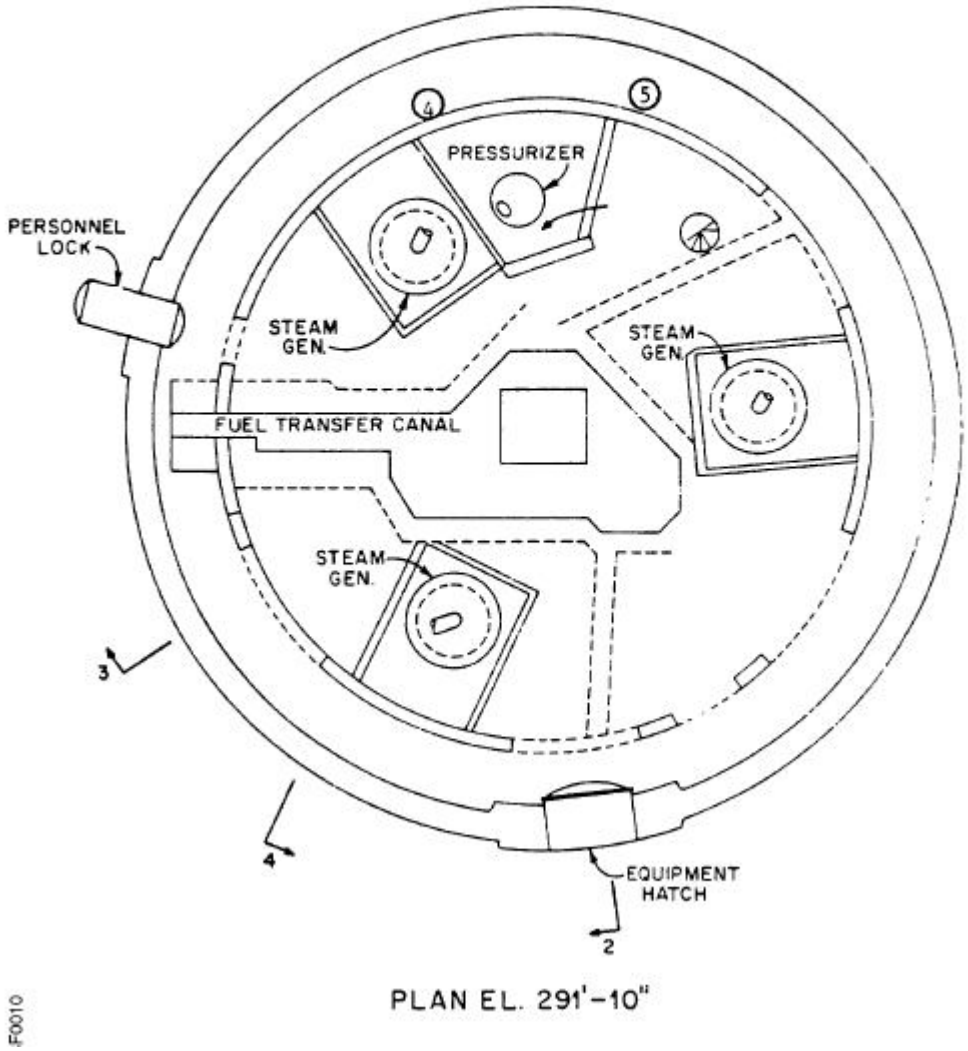

Figure 2: Cross-sectional top view of containment structure from elevation of 291' 10", showing locations of walls, subcompartments, and major equipment [33]. Copyright Dominion Power; Used with permission.

As can be seen in these figures, the wall configuration changes depending on height. This leads to models of the various compartments being subdivided geometrically for analysis. For the purpose of this analysis, the steam generator compartment was analyzed.

In the North Anna UFSAR [1], two analyses are shown to have been initially performed by dividing the subcompartments into seven- and ten-node models. The limiting factor in this particular analysis is the differential pressure between the steam generator compartment and bulk containment. Figure 3 shows that the seven-node model produced the highest differential pressure, and thus was the most conservative model from a safety standpoint. Additionally, Figure 4 shows that in a vertical nodalization scheme, at least five vertical nodes are necessary to meet the most conservative case requirement.

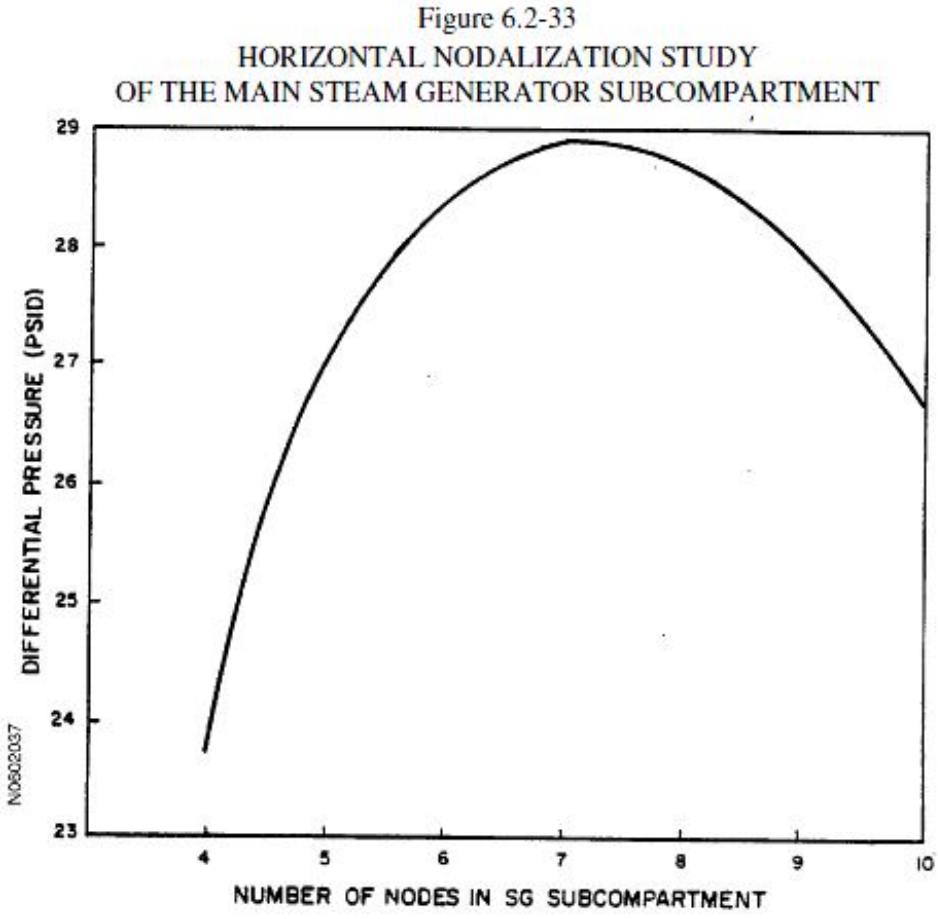

Figure 3: UFSAR graph showing the maximum differential pressure between the steam generator subcompartment and bulk containment as a function of the number of total nodes used in the subcompartment [1]. Copyright Dominion Power; Used with permission.

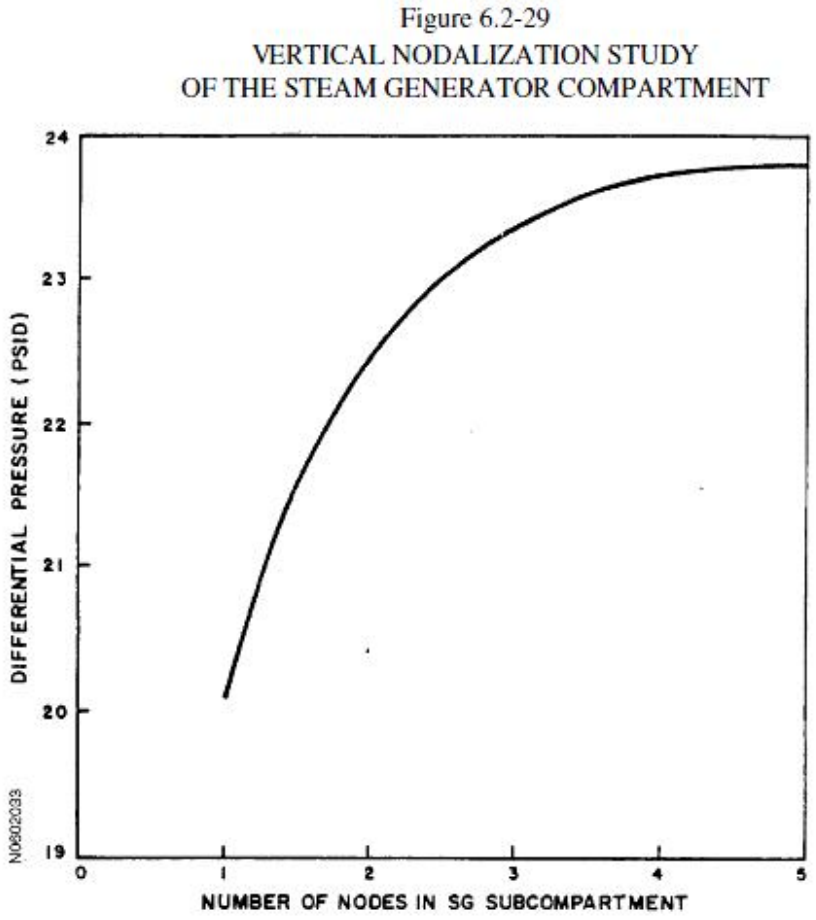

Figure 4: UFSAR graph showing the maximum differential pressure between the steam generator subcompartment and bulk containment as a function of the number of vertical nodes used in the model [1]. Copyright Dominion Power; Used with permission.

The analysis for Figure 3 was performed using a Dominion's nodalization scheme. It would be expected that, depending on how nodalization is performed and if additional nodes were added, the plot may rise again and level off as it approached a different critical pressure.

The analysis was performed by modeling a reactor coolant pipe rupture in the steam generator compartment. Based on the original analysis, a single-ended hot leg break was determined to be

the most limiting break type for this compartment. Mass and energy release data are given in Table 12 in Appendix B.

The compartment is subdivided for analysis using lumped capacitance methods. These subdivisions are determined primarily by geometry, and thus the "wall" of a node may not actually reflect any physical barrier, but merely a geometrically logical breaking point. Figure 5 shows a side view of the steam generator compartment. Logical geometric division locations can be seen at elevations such as 262'-6" and 291'-10". Additionally, Figure 6 shows a cross-sectional top view of the compartment, locations for various nodes are shown to be separated by an imaginary vertical plane that bisects reactor coolant pipes at that elevation of the compartment. Each model also includes three additional nodes. Two of these additional nodes are just outside a wall of the steam generator compartment, and the remaining node is bulk containment. It has been determined that, while walls and obstructions exist within the bulk containment, they will not present enough of a hindrance to affect the average pressure in a volume of the containment's size [1].

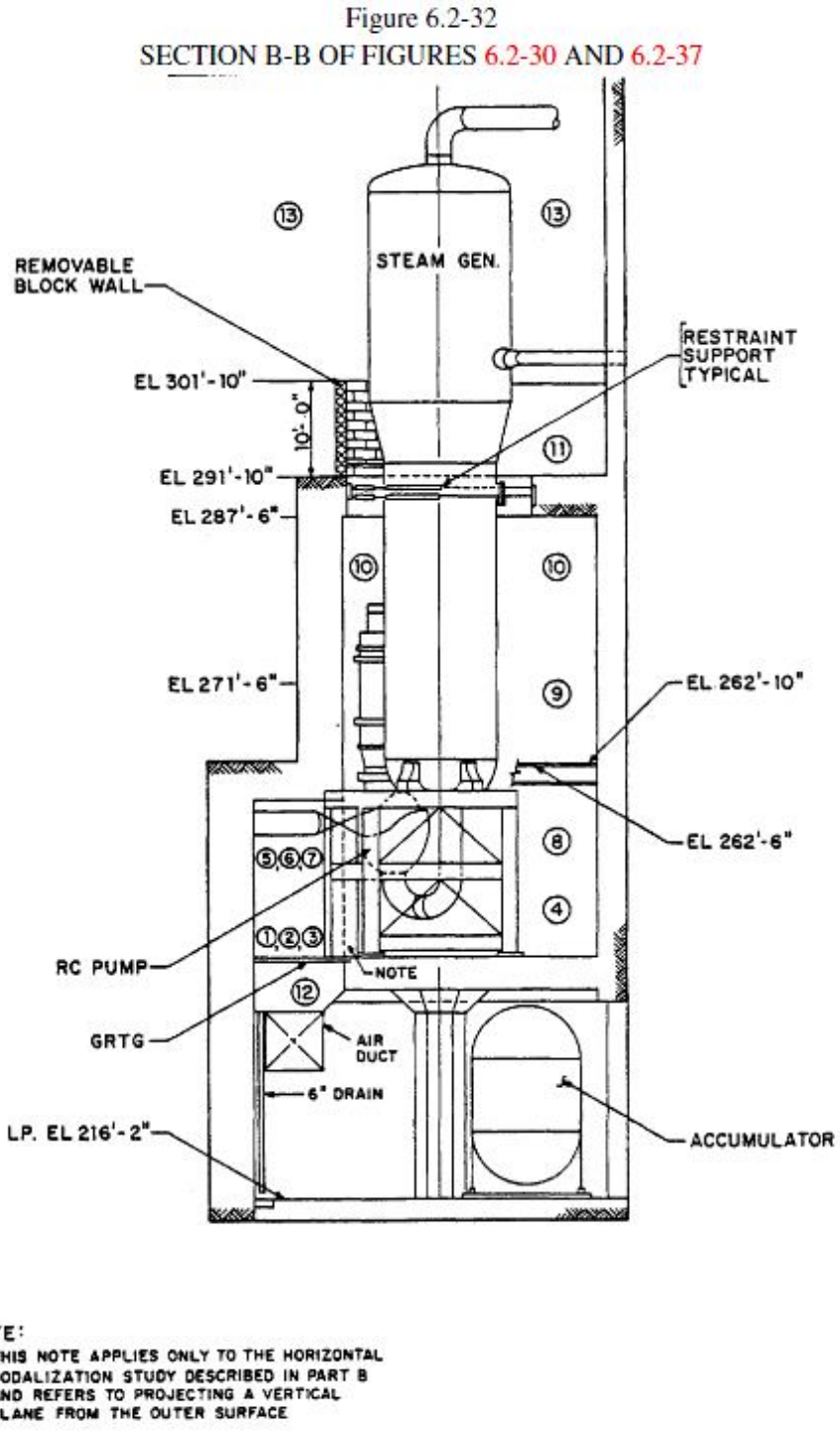

Figure 5: Cross-sectional side view of the steam generator subcompartment, showing nodalization for the 10-node (13 nodes total) model. The model used in the analysis for this thesis was the 7-node model (10 nodes total), which combines the nodes here labeled 5, 6, 7, and 8 into a single node 5 [1]. Copyright Dominion Power; Used with permission.

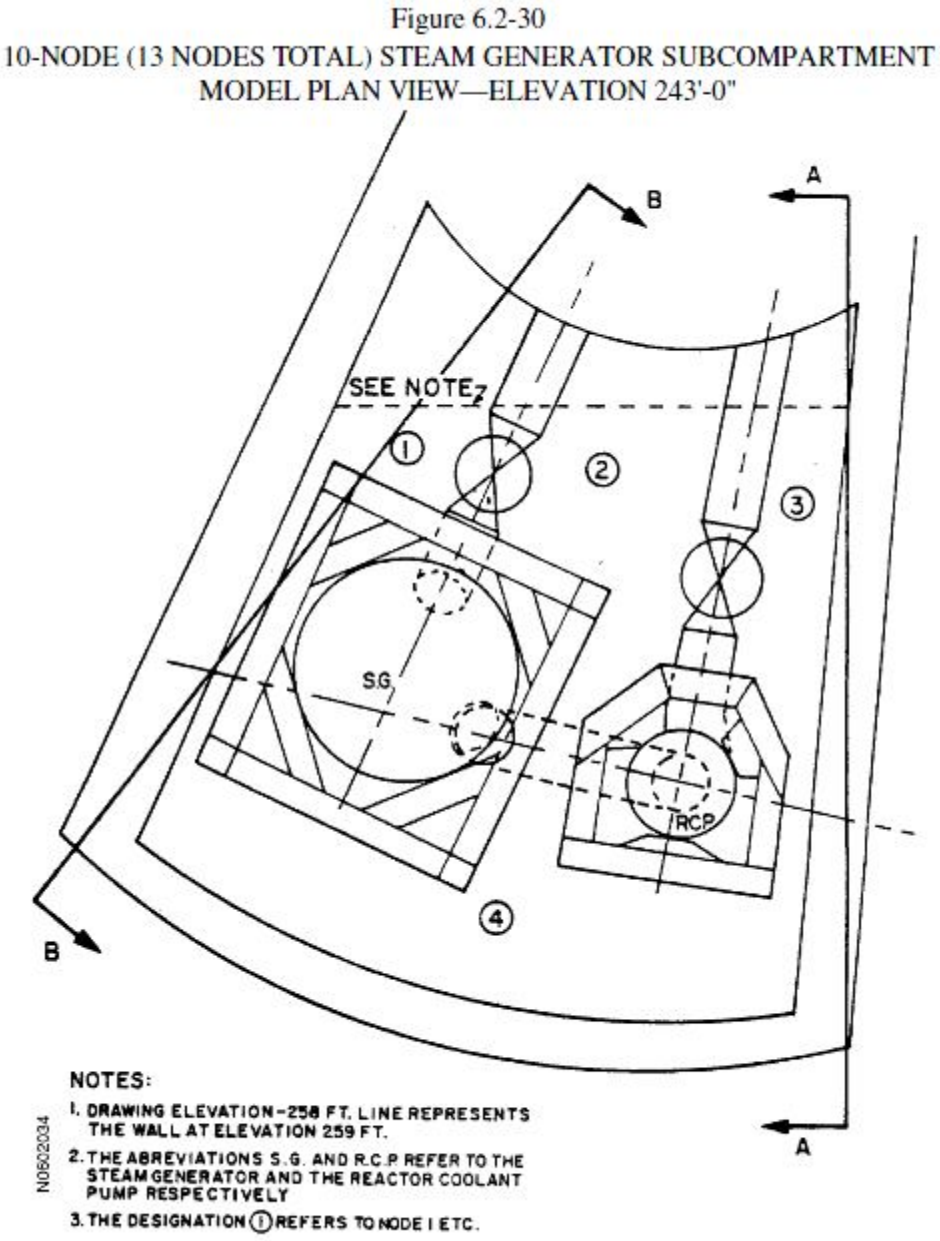

Figure 6: Cross-sectional top view of the steam generator subcompartment at elevation 256', showing the logical geometric divisions creating nodes 1-4. Copyright Dominion Power; Used with permission.

The analysis was performed by postulating a pipe break in the reactor coolant hot leg pipe that feeds into the steam generator between nodes 1 and 2. Thus, flow is assumed to flow equally

into the two nodes. Based on the geometry, it can be noted that these nodes have different cross-sectional areas (and the same height, thus different volumes), so will show slightly different pressures when the same amount of mass and energy flow into each node [1].

The nodalization for the 7-node model is given by Figure 7, which shows a block diagram with many of the flow paths between nodes. It is organized by elevation. For a complete accounting of all flow paths and their respective parameters, refer to Table 8 in Appendix A.

Figure 6.2-35
7-NODE MODEL (10 NODES TOTAL)
NODAL ARRANGEMENT FOR THE STEAM GENERATOR SUBCOMPARTMENT

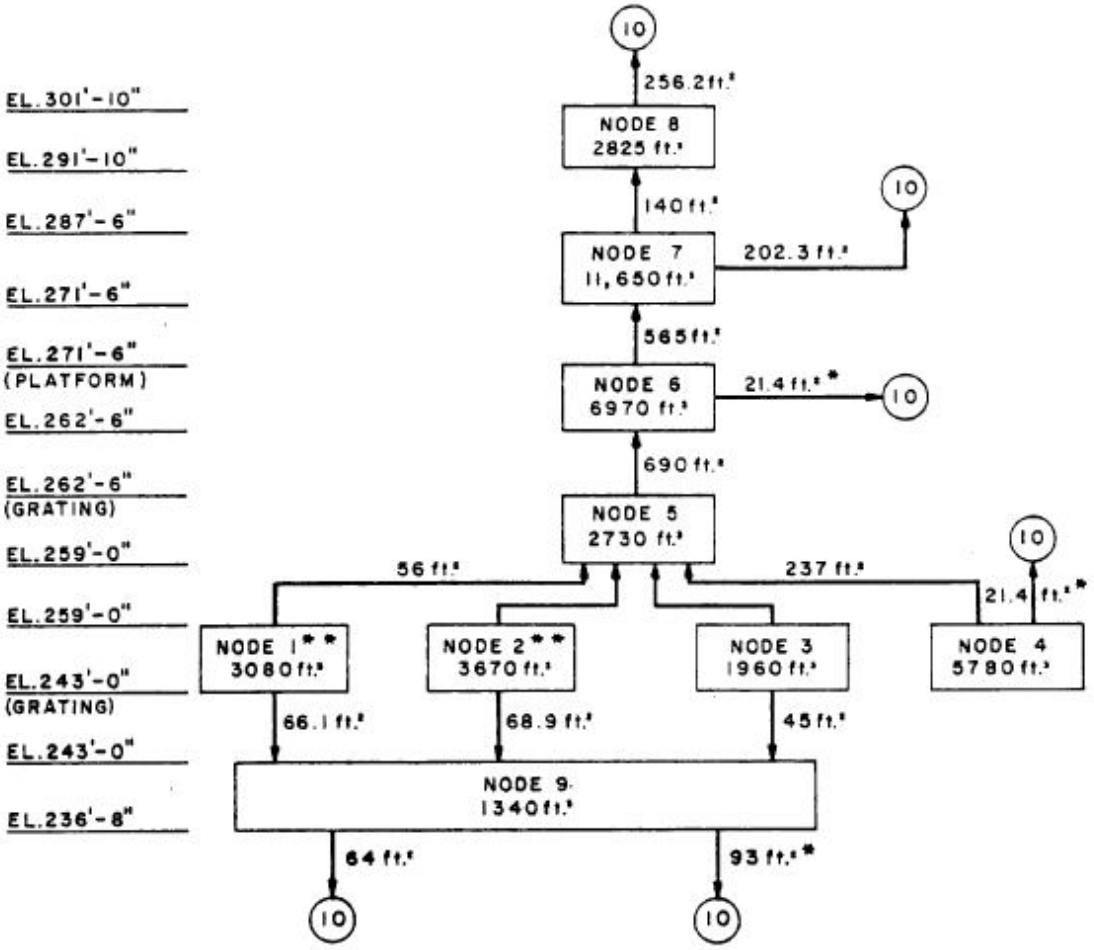

Figure 7: Block diagram for the 7-node steam generator subcompartment model. Note that not all flow paths are shown between nodes 1-4 [1]. Copyright Dominion Power; Used with permission.

The results of the UFSAR analysis of the 7-node model are shown in Figure 8.

Figure 6.2-34
7-NODE MODEL DIFFERENTIAL PRESSURE BETWEEN THE STEAM GENERATOR SUBCOMPARTMENT (ELEVATION 243'- 0" TO ELEVATION 287'-6") AND THE CONTAINMENT VERSUS TIME AFTER ACCIDENT

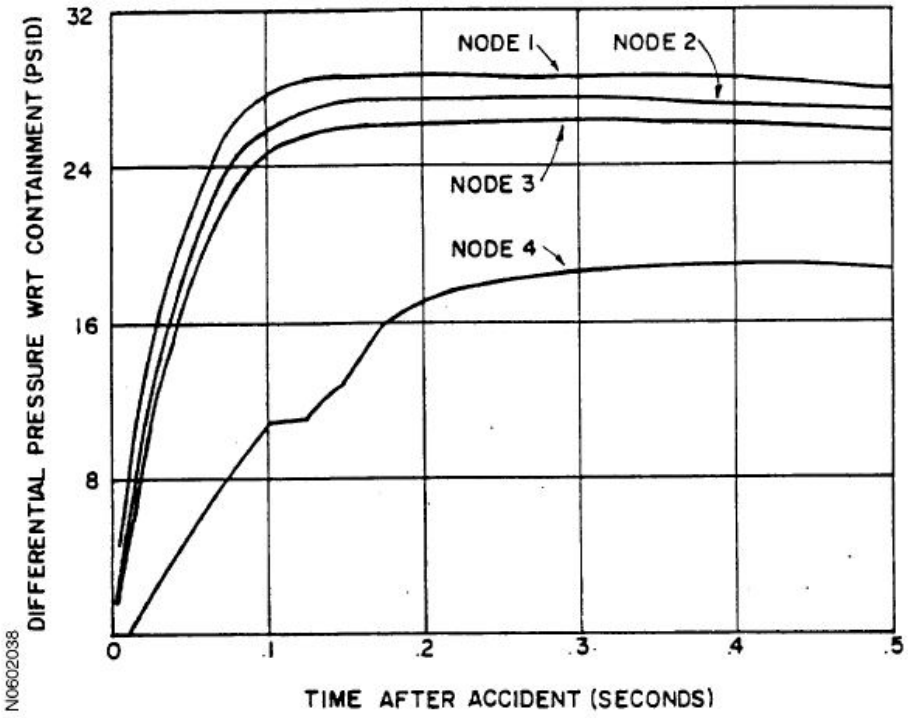

Figure 8: UFSAR graph of differential pressures between nodes 1-4 and bulk containment [1]. Copyright Dominion Power; Used with permission.

The approximate maximum differential pressures shown in Figure 8 are summarized in Table 1 below.

Table 1: Maximum differential pressures in nodes 1-4 for the UFSAR model. Note that these values are approximate.

UFSAR Maximum Differential Pressures (Approximate)

Node	Max Pressure (psid)
1	28.9
2	27.7
3	26.3
4	19.4

While the model consists of ten total nodes, nodes 1 to 4 presented the highest differential pressures with respect to bulk containment. Node 1 shows the highest differential pressure, topping out at about 29 psid. The transient time on this analysis is 0.5 seconds, though differential pressure values reach a steady-state after about 0.2 seconds. By this time, blowout panels have been expelled, and fluid flow has commenced through all flow paths [1]. While fluid will continue to flow after differential steady state has been achieved, overall containment pressure over about an hour transient is beyond the scope of this analysis.

The calculations that were performed by Dominion Power with the assistance of Westinghouse Nuclear are based on a proprietary set of models and equations. These calculations utilized a combination of computer aided solving and solutions obtained by written formulas. Ultimately, they have been accepted by Dominion and the US. Nuclear Regulatory Commission, and so will be considered an appropriate benchmark for the purpose of this thesis.

3 Simulation Setup

3.1 Benchmarked Model

The first step in creating an equivalent model in GOTHIC (version 8.0) was to create a model that could be compared to known quantities. Once the initial GOTHIC model was created, it could be benchmarked against the results of the UFSAR model. After a benchmarked model was created, it could then be altered to create models of different configurations.

Figure 9 shows the nodalization diagram for the GOTHIC base case, which will use the existing UFSAR model as a benchmark. This can be compared to Figure 7, which is the UFSAR nodalization diagram.

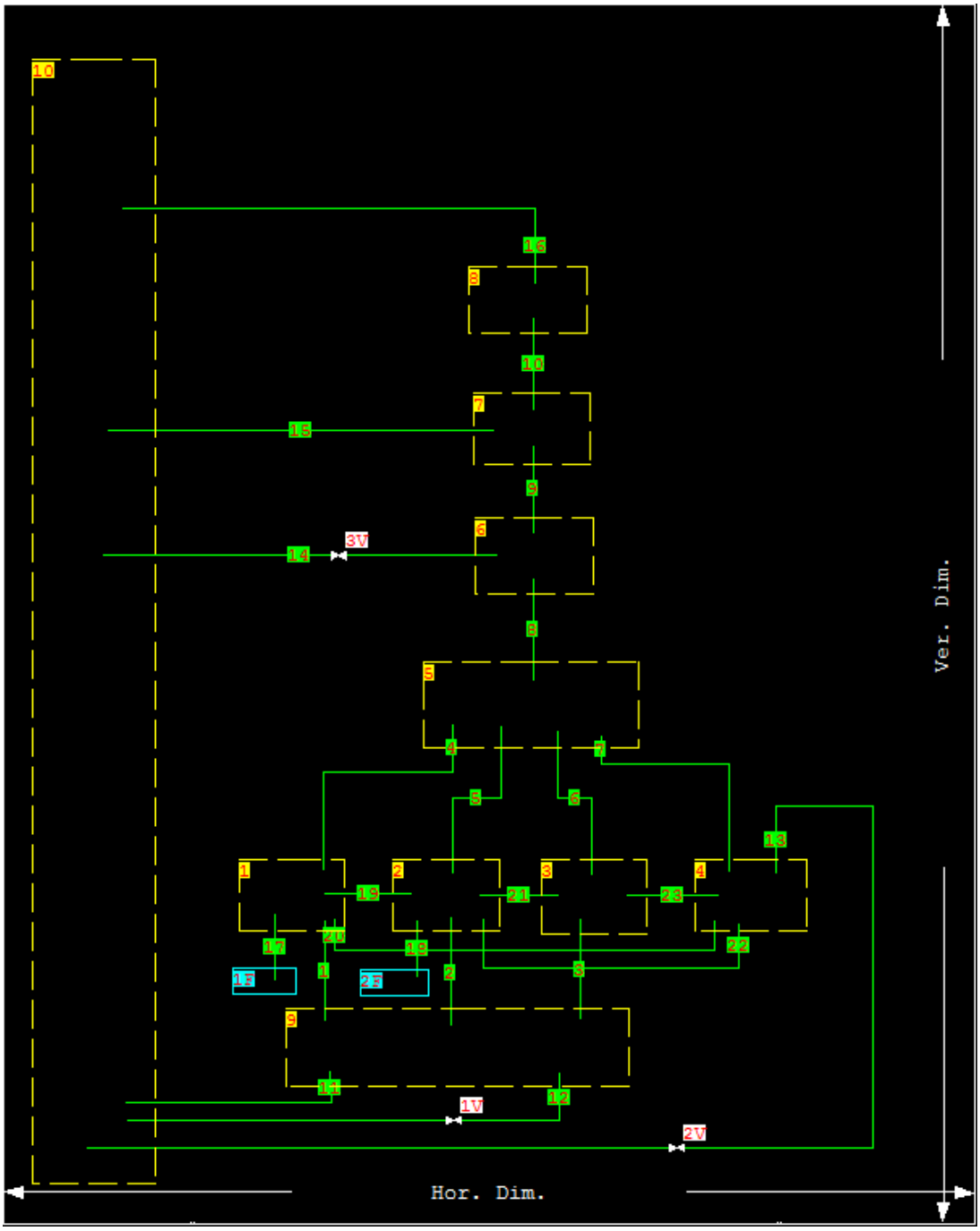

Figure 9: GOTHIC nodalization diagram for the base case.

The figures are nearly identical. Notable additions to the GOTHIC diagram are the flow boundary conditions, which are indicated by a double-asterisk in the UFSAR diagram, and

blowout panels, which are represented as valves in the GOTHIC diagram and as a single-asterisk in the UFSAR diagram. Additionally, there are flow paths between nodes 1 to 4 which are not shown on the UFSAR diagram, but are described in Table 8 in Appendix A.

Once complete, the GOTHIC model was compared to the UFSAR model. The primary metric for comparing the GOTHIC model to its UFSAR benchmark was differential pressure between nodes 1 to 4 and bulk containment. The UFSAR shows differential pressures in Figure 8.

Since there is significant buildup of pressure within nodes, it can be suspected that the flow paths are considerably constricting free flow, and thus creating critical flow. This was corroborated by GOTHIC output. The Homogeneous Equilibrium Model (HEM) was chosen to model the critical flow for this simulation. Since most of the flow paths are very short as compared to their diameters, thermodynamic effects will be have a minimal effect on the fluid. Additionally, because GOTHIC is able to recalculate representative variables very quickly and the because the flow will transcend the flow restrictions in a very short time, a homogeneous approach is acceptable.

Matching the GOTHIC model to the UFSAR model was a necessary step to allow for the nodalization study to be performed. The creation of a controlled model established a basis for comparison between that and the UFSAR model, which provided for more direct evaluation of the nodalization study.

Figure 10 shows the GOTHIC results base model. Additionally Figure 11 shows the absolute pressures from GOTHIC.

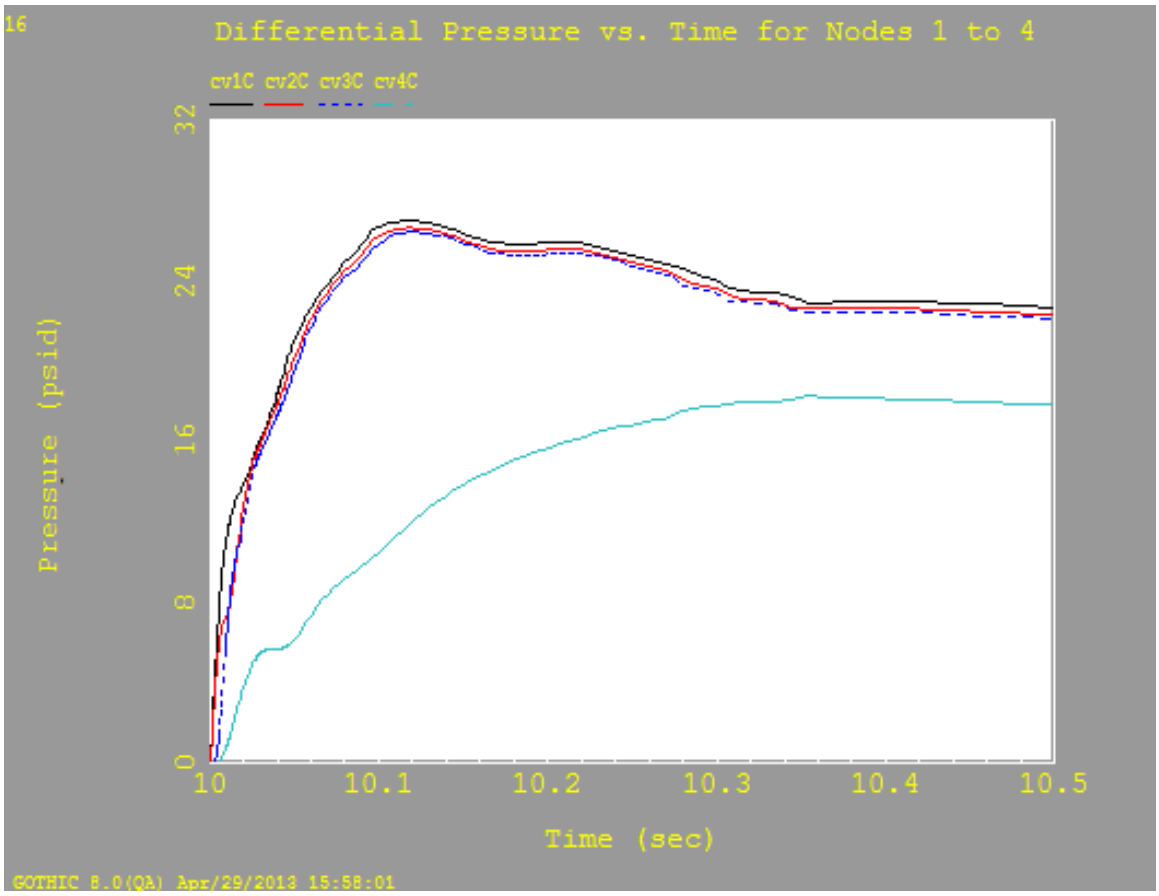

Figure 10: Differential Pressure v. Time for nodes 1-4 between respective nodes and bulk containment node for the base model. The lines labeled cv#C apply to the node indicated (i.e. cv1C refers to the differential pressure between node 1 and the bulk containment node).

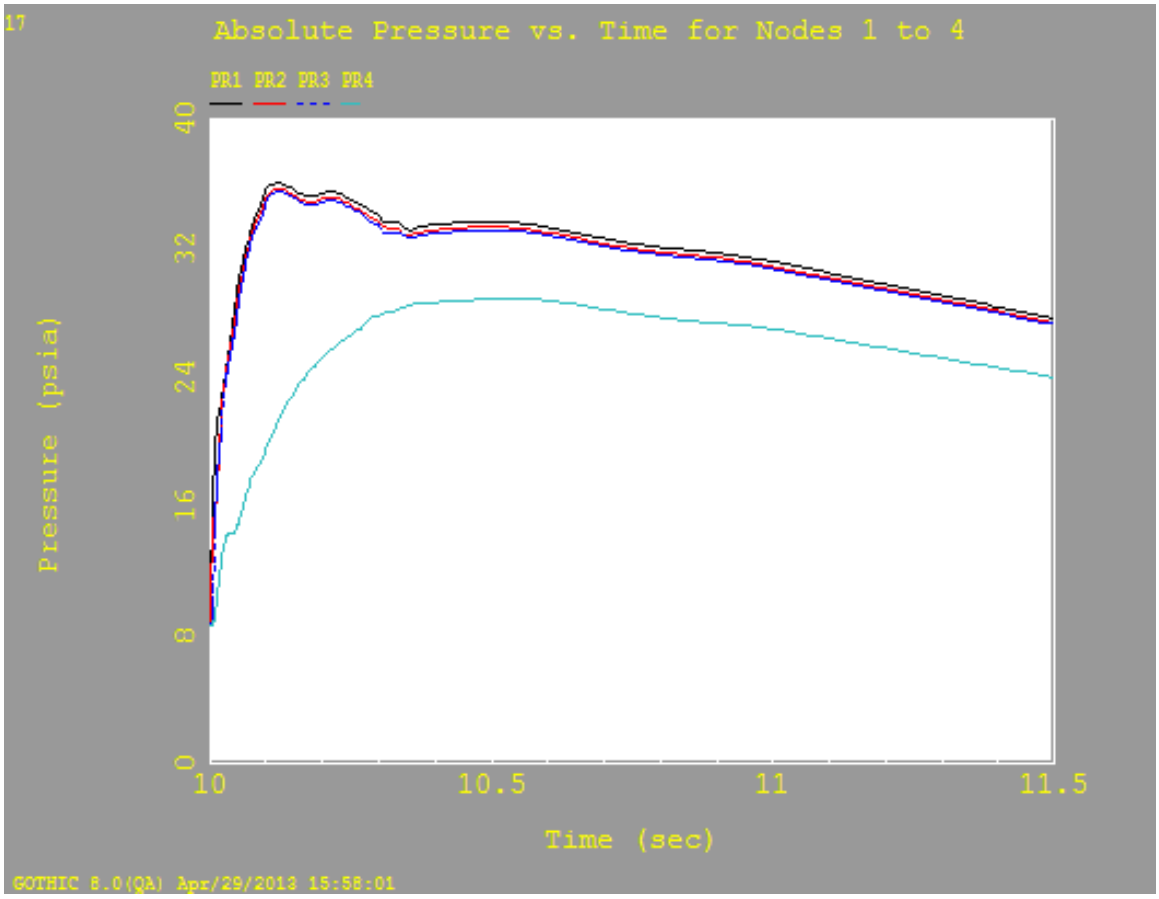

Figure 11: Absolute Pressure v. Time for nodes 1-4. The lines labeled PR# apply to the node indicated (i.e. PR1 refers to the absolute pressure in node 1).

It is notable that the GOTHIC plots produced for this thesis were from models which all employed a null transient. A null transient is intended to show that the model is at a steady state before the beginning of the intended model actions. Thus, all GOTHIC plots shown here begin after a 10 second null transient.

Table 2 shows the maximum differential pressures for this model, summarized from Figure 10.

Table 2: Maximum differential pressures in nodes 1-4 for the original base model.

Original Model Maximum Differential Pressures

Node	Max Pressure (psid)
1	27.01
2	26.65
3	26.43
4	18.28

The plots for this model show a maximum differential pressure of 27.01 psid and a maximum absolute pressure of 36.06 psia. Compared to the UFSAR's max differential pressure of around 28.7 psid, there appears to be about a 6% difference between the models. As can be observed in Figure 8, the plot appears to be hand-drawn, so the pressures indicated may be approximate to the scale given, and there may be significantly less than the approximated 6% difference. Regardless, the results of the GOTHIC model are close enough to be considered accurate for the purpose of establishing a baseline for experimentation.

In comparing Figure 8 and Figure 10, the general trends of the graph are very similar. The differential pressure lines for nodes 1 to 3 stay very close together, rising sharply in the first 0.1 second, and then leveling off. The differential pressure line for node 4 rises gradually, with a disruption around 0.1 second.

Minor differences between the graphs exist in the peak differential pressure for node 4, which in Figure 8 is about 19.4 psid, and in Figure 10 is only about 18.28 psid, and the fact that the differential pressures for nodes 1 to 3 decrease by about 4.3 psid toward the end of the transient in Figure 10.

The former is likely due to the configuration of the blowout panel valves in the GOTHIC model. The blowout panels were modeled as quick-open valves. The valve/door option in GOTHIC most closely represented a blowout panel. Realistically, however, there would be an opening travel curve with associated additional loss coefficients and other variables, but this data was unavailable in the UFSAR, so a standard quick-open valve type was the best option. The configuration of the blowout panels would likely also affect the disruption in the node 4 curve, which happens before 0.1 second in the GOTHIC plot, but after 0.1 second in the UFSAR plot.

The latter difference is beginning to show some pressure equalization between the nodes and bulk containment. It is unclear whether this is an oversight in the UFSAR graph (again since it appears to be hand-drawn) or if this is a legitimate difference between the UFSAR model and the GOTHIC model. However, since peak pressure is the variable of interest, these lower pressures are not germane to this analysis.

As expected, the graphs for differential pressure and absolute pressure show similar trends. Near the beginning of the transient, they are separated by the initial pressure in containment (about 9 psia). Because bulk containment is so much larger, its pressure is not affected as quickly by the hot leg break as the local compartment's pressure. The absolute pressure graph displays the full 1.5 second transient, which shows the pressures from nodes 1 to 5 converging as flow out of the reactor coolant system decreases, and a downward trend in the pressures as they begin to equalize with bulk containment.

3.2 Decreased Nodalization

Since Figure 10 indicates that node 1 has the highest pressure, it is the focus point of model adaptation. In order to examine the effects of various levels of nodalization, it was necessary to first combine nodes. Node 2, being the closest to node 1 in location and pressure was the logical choice for this combination.

As Figure 6 shows, nodes 1 and 2 are separated by a geometrical feature, which is the hot leg pipe which is postulated to break. For modeling purposes, the flow from the hot leg pipe break is split equally between these two nodes. It is therefore reasonable to combine these two nodes into a single node, and to set the flow from the pipe break to flow completely into the combined node. The nodalization diagram for this case from GOTHIC is shown in Figure 12 below.

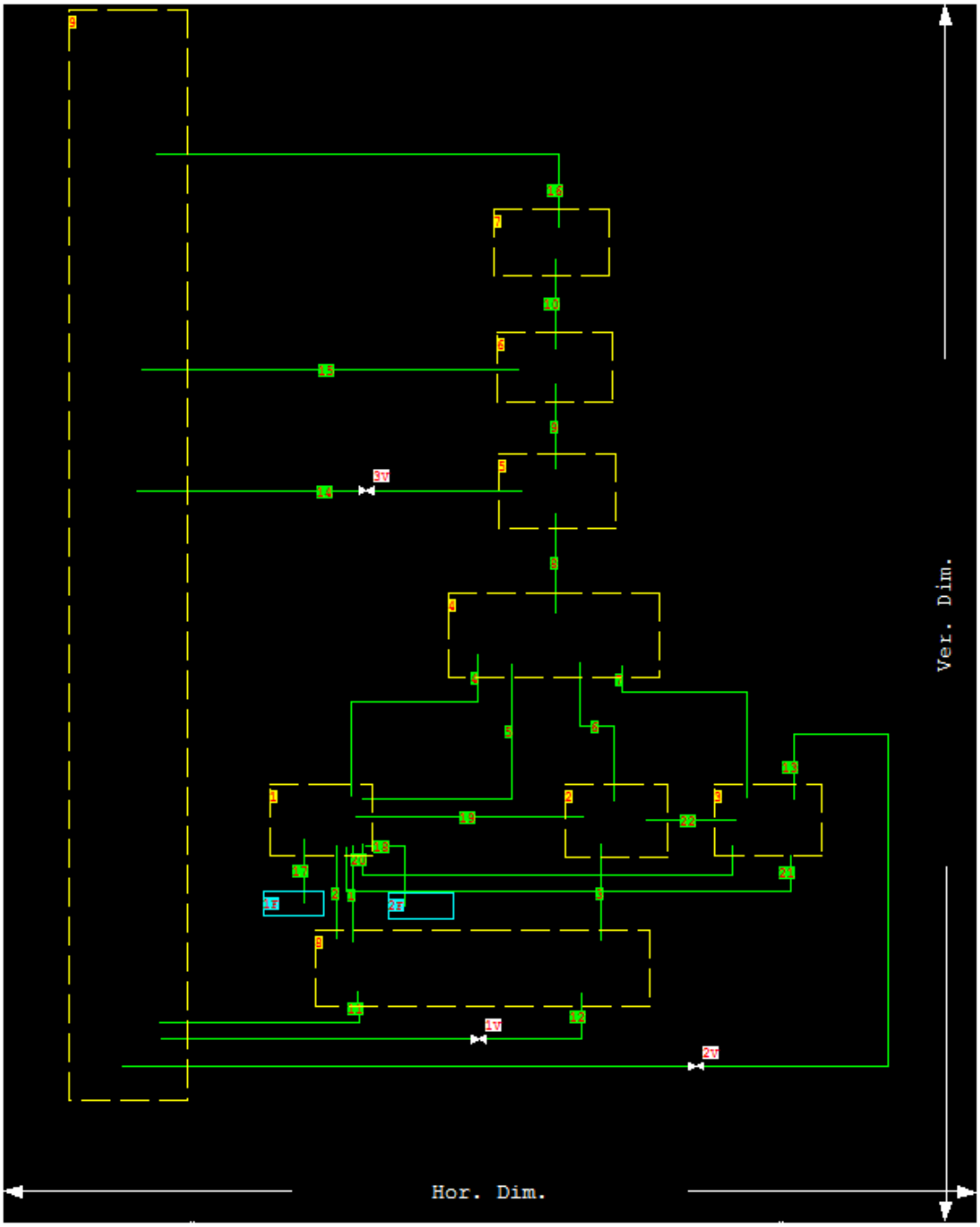

Figure 12: Nodalization diagram for case of combined nodes 1+2.

As can be seen in comparison to Figure 9, the alterations made to the original nodalization diagram were relatively small. They involved shifting the overall volume from node 2 into node

1, creating a new overall volume of 6750 ft^3 for node 1. Then, the flow path between nodes 1 and 2 was removed, and all other flow paths that were connected to node 2 were shifted to connect to node 1. In this manner, the flow paths are held to a constant effect on the model and no scaling factors need to be considered. Results of this nodalization change will be discussed in Chapter 4.

3.3 Increased Nodalization

It is hypothesized that the model created for the UFSAR was oversimplified to accommodate the computational technology of the time it was created. To test this, additional nodes were added to the benchmark model in order to determine the results.

Once again, node 1 is the node of interest. It was subdivided into nine equally-sized sub-nodes in the x-y plane. The z-plane has not been subdivided in order to maintain a constant cell height between the subdivided node and adjacent nodes and since Figure 3 indicates that there would likely be no benefit at this time. The subdivision diagram is shown in Figure 13 and sub-node assignments are shown in Figure 14 below.

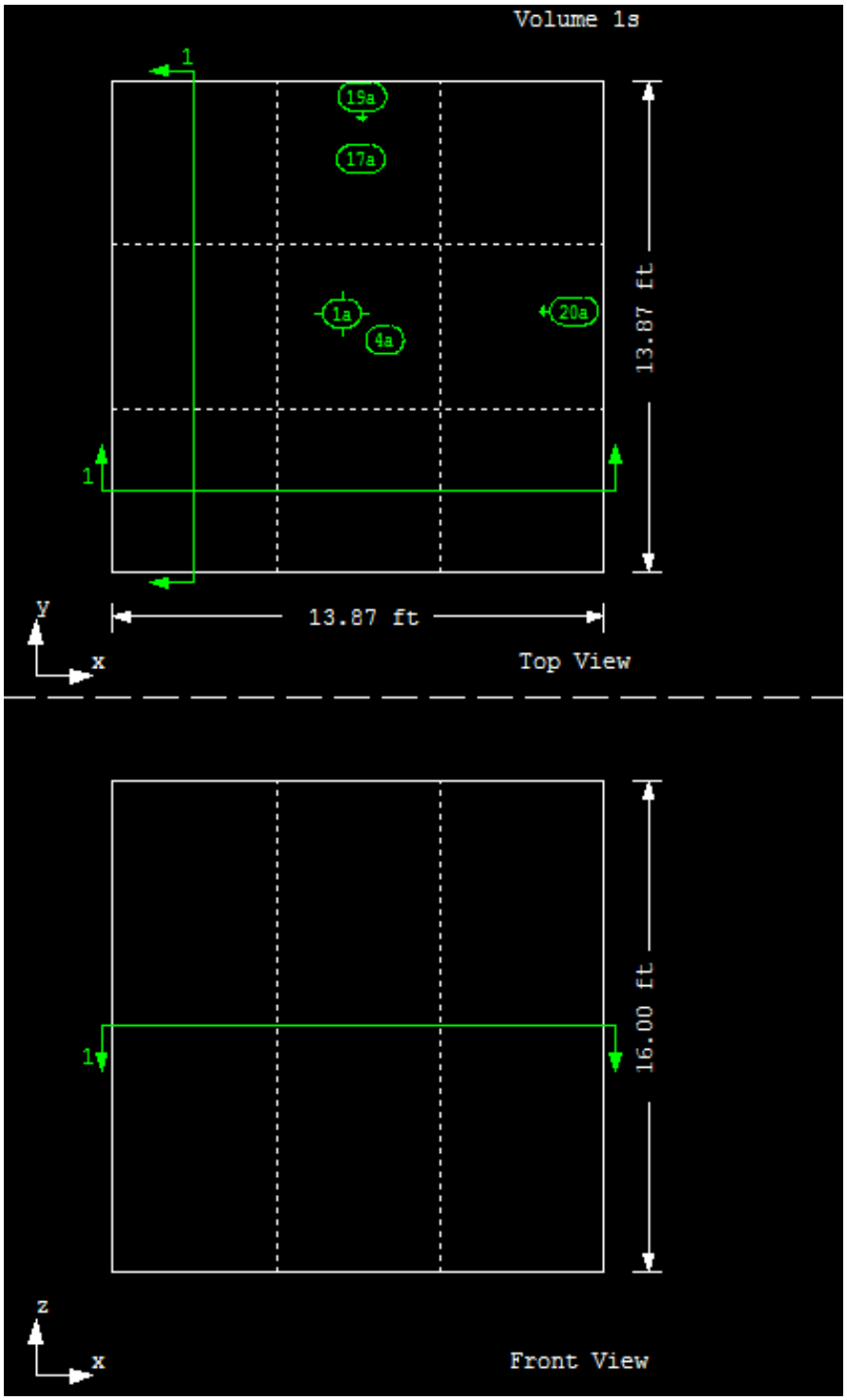

Figure 13: Diagram of node 1, subdivided into 9 sub-nodes.

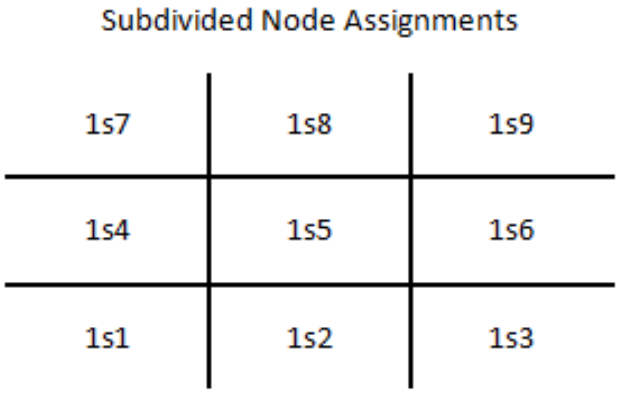

Figure 14: Subdivided node assignments within node 1. The format is given by node #, an 's' denoting a subdivision, and sub-node # (GOTHIC assigns these designations).

In order to match the geometry of the original model, flow paths have been connected to appropriate sub-nodes. This may be compared to Figure 5 and Figure 6. Flow path 19 connects to node 2 through the side of sub-node 1s8, flow path 20 connects to node 4 through the side of sub-node 1s6, flow path 1 connects to node 9 through the bottom of sub-node 1s5, and flow path 4 connects to node 5 through the top of sub-node 1s5. Flow path 17 represents the hot leg pipe break, which is in sub-node 1s8. Since the hot leg pipe is the geometric feature that divides nodes 1 and 2, the pipe break must be located along the side of node 1 that is shared by node 2. Since flow paths in GOTHIC can only be attached to one sub-node, each flow path has been located centrally to the side of node 1 to which it is attached.

It is important to note that the modification being modeled here is distinctly different than that in Figure 4, which examines the conservative nature of the model with respect to the total number of nodes within the subcompartment. Since this modification does not rearrange or change the respective volumes in any but one node, the overall conservatism of this experiment should not

differ from the UFSAR model. However, the relative layouts used to produce Figure 4 are not given in the UFSAR, so it may be beneficial in the future to analyze the effects of rearranging the nodes and attempting to justify a less conservative but potentially more accurate model.

4 Results and Discussion

4.1 Decreased Nodalization

The results of the case where nodes 1 and 2 were combined ultimately showed that there was only a small difference between this case and the original model. This is likely due to slight volume differences between the two cases.

Figure 15 and Figure 16 below show the differential pressures and absolute pressures, respectively.

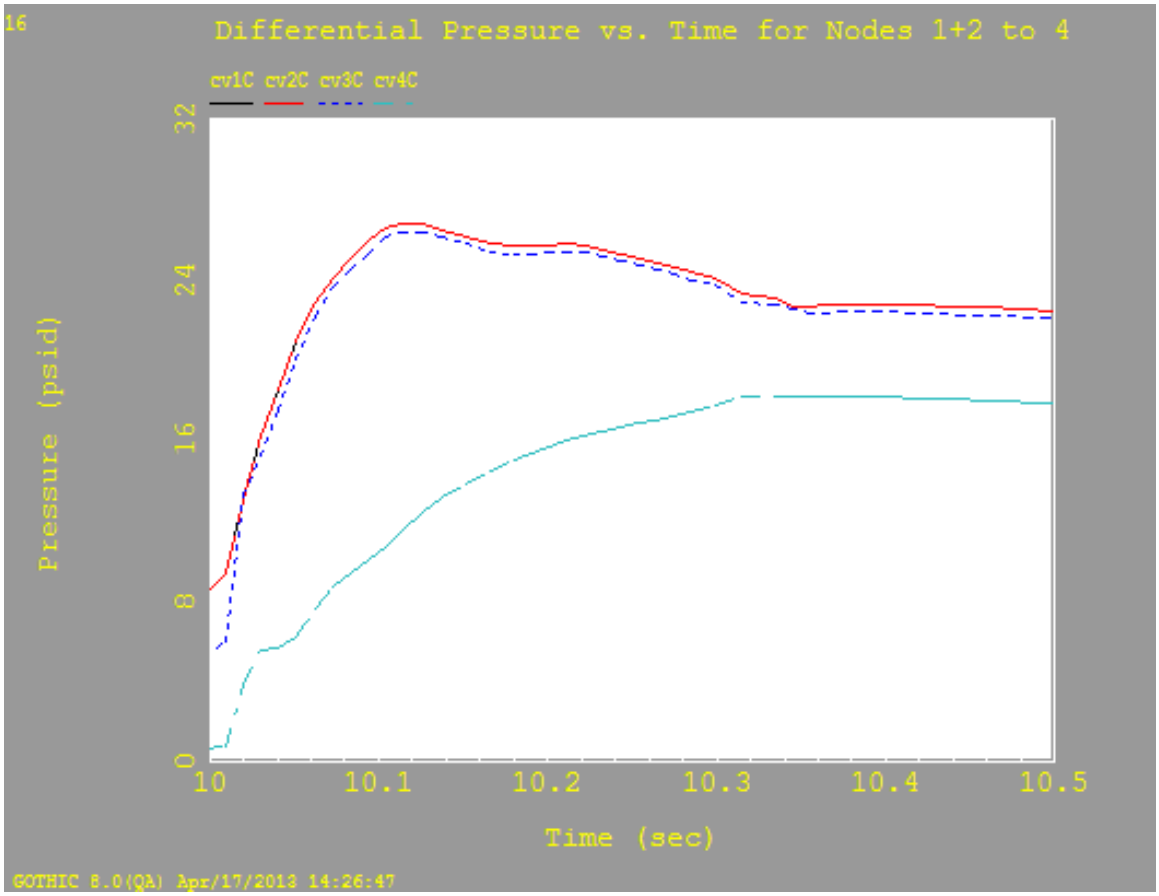

Figure 15: Differential Pressure vs. Time for combined nodes 1+2 - node 4 between respective nodes and bulk containment node. The lines labeled cv#C apply to the node indicated (i.e. cv1C refers to the differential pressure between node 1 and the bulk containment node). cv1C and cv2C both apply to the combined node 1+2 in this case, and are thus identical.

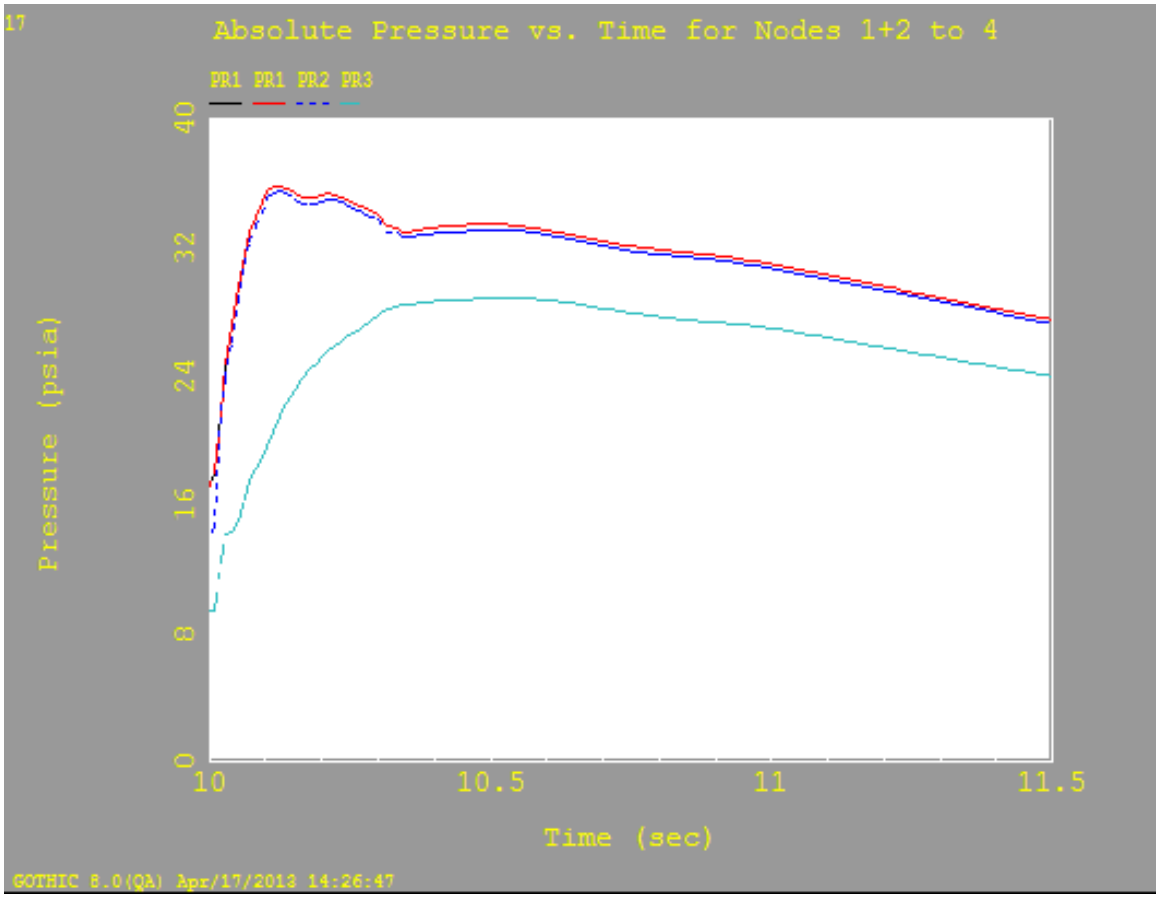

Figure 16: Absolute Pressure vs. Time for combined nodes 1+2 - Node 4. The lines labeled PR# would generally apply to the node indicated (i.e. PR1 refers to the absolute pressure in node 1), but since the original node 2 was removed, PR2 and PR3 actually refer to the pressures in original nodes 3 and 4. PR1 is displayed twice for graph consistency with regard to the combined node 1+2.

Table 3 shows the maximum differential pressures for this model, summarized from Figure 15.

Table 3: Maximum differential pressures in nodes 1+2-4 for the combined nodes model.

Combined Nodes Model
Maximum Differential Pressures

Node	Max Pressure (psid)
1+2	26.8
3	26.42
4	18.23

Ultimately, both graphs show approximately a 0.5 psi decrease in pressure after combining the two nodes. Figure 15 shows a maximum differential pressure of 26.80 psid, and Figure 16 shows a maximum absolute pressure of 35.88 psia. These can be compared with maximum pressures of 27.01 psid and 36.06 psia in Figure 10 and Figure 11, respectively.

The reason that the pressures are slightly lower likely is related to the way that GOTHIC calculates volume parameters. GOTHIC assumes that all volumes have a square base with four walls, given a set volume, height, and hydraulic diameter [34]. When the walls between nodes 1 and 2 are removed and the volumes are combined, some flow restrictions are removed and the wetted area is reduced. GOTHIC has the ability to adjust for this, if given more information than was available in the UFSAR.

In the end, however, the change in pressure between the cases is nearly negligible. This is what would be expected for the given conditions. Since the original pressure is slightly higher, it satisfies the condition of being more limiting and conservative, as required for regulatory approval, and is thus the model that is used. The reason for testing the combined nodes model was to check the opposite effects of the increased-nodalization hypothesis to help validate the possible results.

4.2 Increased Nodalization

The case of increased nodalization produced much more complex results than other cases, but yielded applicable detail. Specific placement of the hot leg pipe break changes the distribution of pressure within node 1, which in turn affects the adjoining nodes.

Figure 17 and Figure 18, below, show the pressures in each subdivided node.

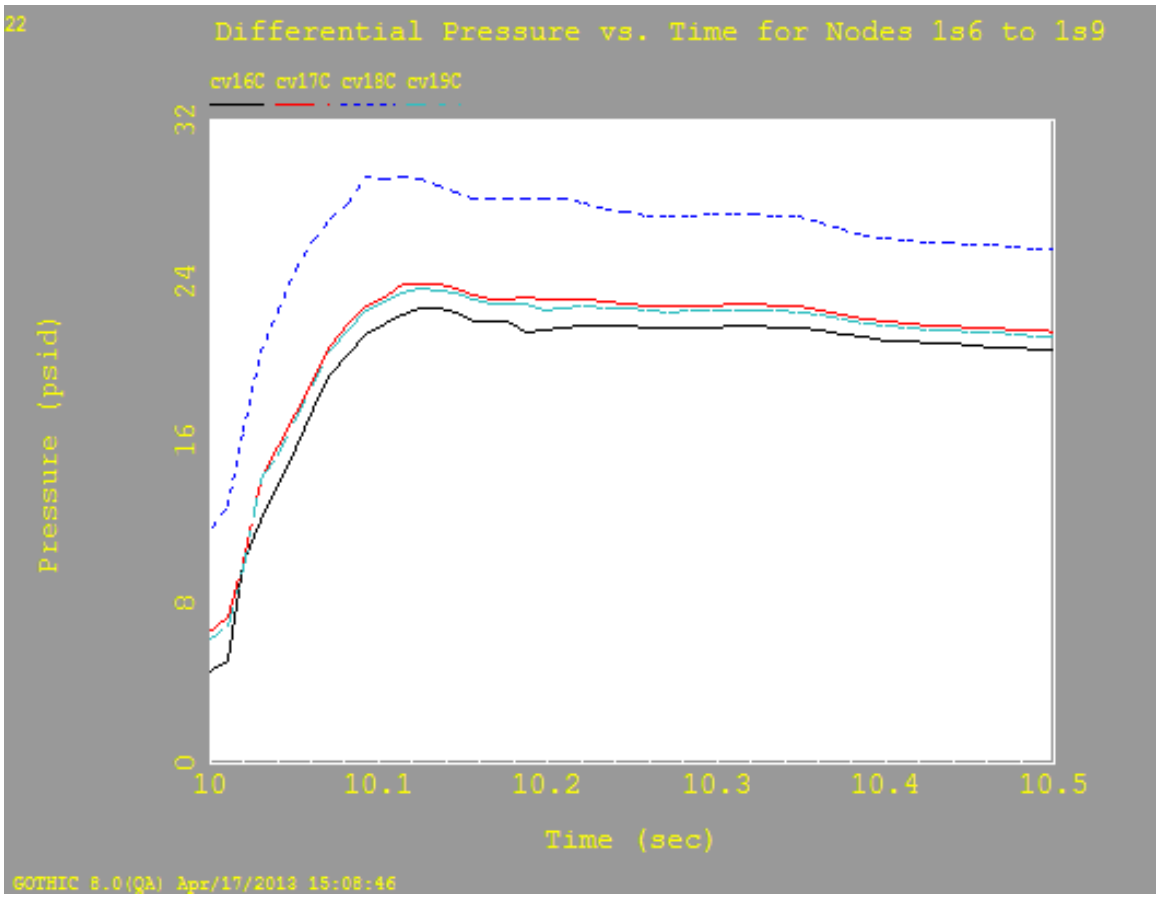

Figure 17: Differential Pressure vs. Time for Nodes 1s6-1s9. Here, cv16C refers to the differential pressure in sub-node 6, cv17C to sub-node 7, cv18C to sub-node 8, and cv19C to sub-node 9.

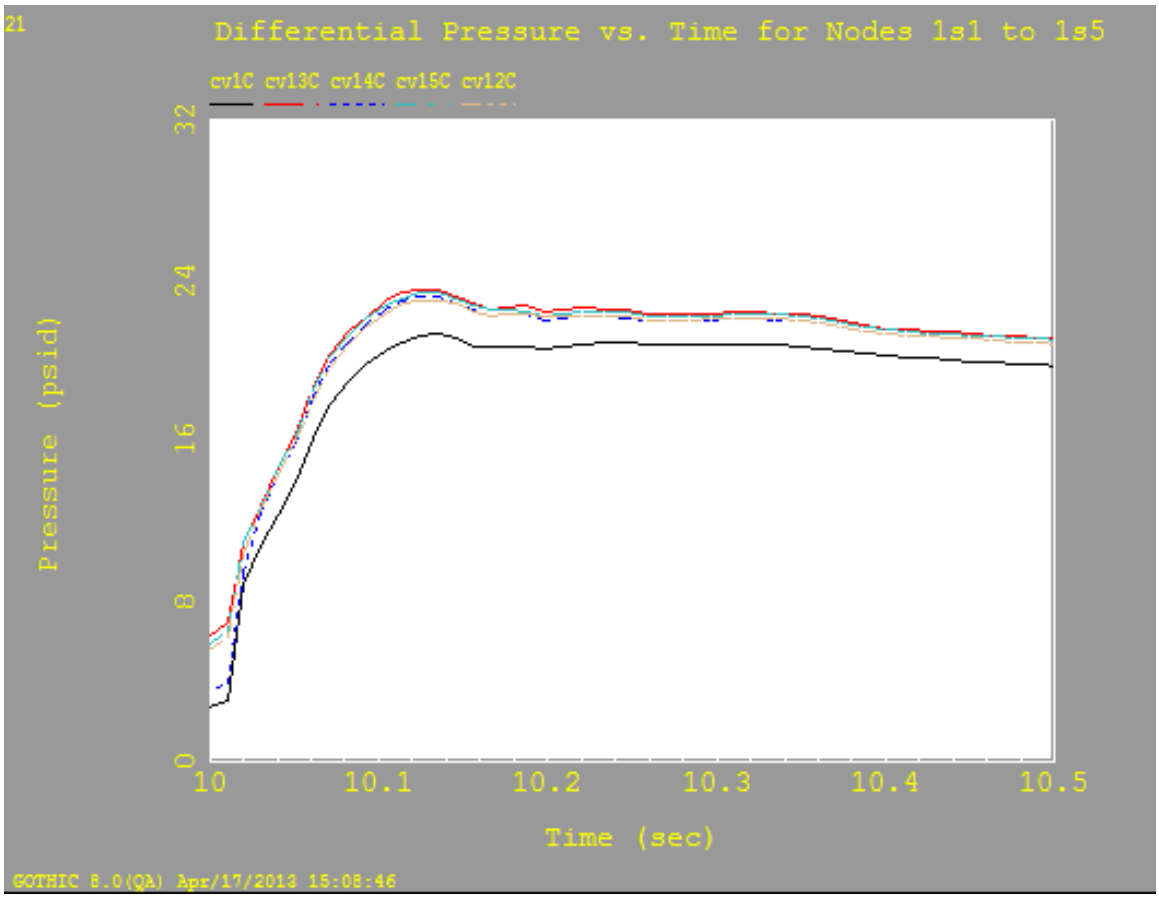

Figure 18: Differential Pressure vs. Time for Nodes 1s1-1s5. Here, cv1C refers to the differential pressure in sub-node 5, cv13C to sub-node 1, cv14C to sub-node 2, cv15C to sub-node 3, and cv12C to sub-node 4.

Table 4 shows the maximum differential pressures for this model, used in Figure 18, Figure 19, Figure 20, and Figure 21.

Table 4: Maximum and average (as noted) differential pressures for nodes 1s1-1s9 and 2-4.

Subdivided Model Maximum Differential Pressures

Node	Max Pressure (psid)
1s1	23.54
1s2	23.18
1s3	23.42
1s4	23.05
1s5	21.33
1s6	22.67
1s7	23.86
1s8	29.21
1s9	23.62
2	28.42
3	28.2
4	18.31
Avg 1s1-1s9	23.76
Avg 1s1-1s7, 1s9	23.08

As can be seen in these figures, the pressures in most sub-nodes are about the same (between 22.6-23.9 psid), with two notable exceptions. Sub-node 1s5 (Figure 18, line cv1C) displays understandably low pressures since this node has two exit flow paths to other nodes. With additional area, there is less mass buildup in this node. Conversely, sub-node 1s8 (Figure 17, line cv18C) shows significantly higher pressures than any other sub-node. Even though this sub-node contains an exit flow path, the combination of high energy and volume of liquid from the hot leg pipe break and high pressures on the back side of that exit flow path cause a localized buildup of pressure and force the fluid into adjacent sub-nodes. For a rough idea of the shape of the pressure distribution and how this compares to the case that was not subdivided, see Figure 19.

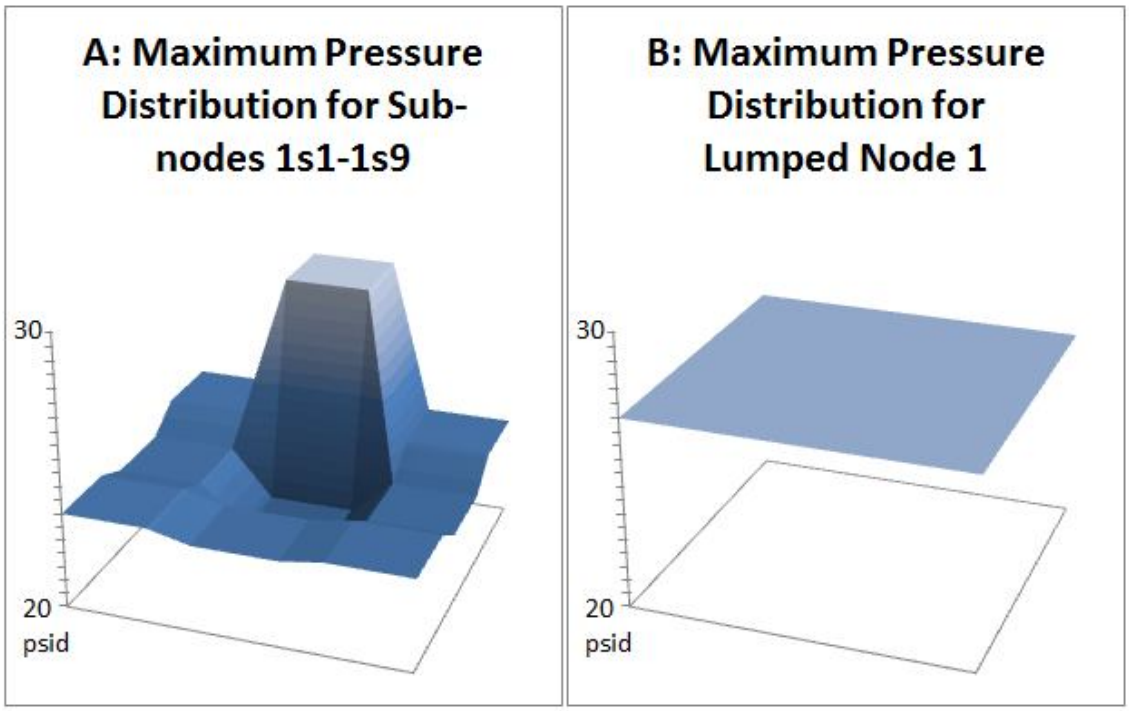

Figure 19: Subplot A shows the Maximum Pressure Distribution for sub-nodes 1s1-1s9. 1s1 is in the corner nearest the z-axis, and Figure 14 shows the layout of the sub-nodes. Subplot B shows the Maximum Pressure Distribution for Lumped Node 1.

These graphs show the difference in the detail that sub-nodalization can provide. Because GOTHIC calculates each model using the lumped capacitance method, it assumes that the maximum pressure is the average pressure within the node and is constant throughout that node. In actuality, there is a pressure spike around the pipe break that can only be observed with sub-nodalization. However, as expected, the average pressure in the other adjacent sub-nodes is lower than the previously-calculated average.

This large differential pressure around the pipe break makes that sub-node one of great interest. As stated, the pipe break was assumed to be central to the side of the node, but this is not necessarily true. Realistically, a pipe could break in any location. Since the local pressure dissipates quickly as it travels away from the break, it is uncertain what the effect might be if the

pipe break were located in a node that was adjacent to a pressure-sensitive wall. The local pressure may be enough to affect the wall, or the wall may act to redirect the pressure without damage, since there is little resistance to flow in directions away from the node wall.

To provide a basis for comparison to other cases, Figure 20 shows the equivalent graph to Figure 8, as given for each case.

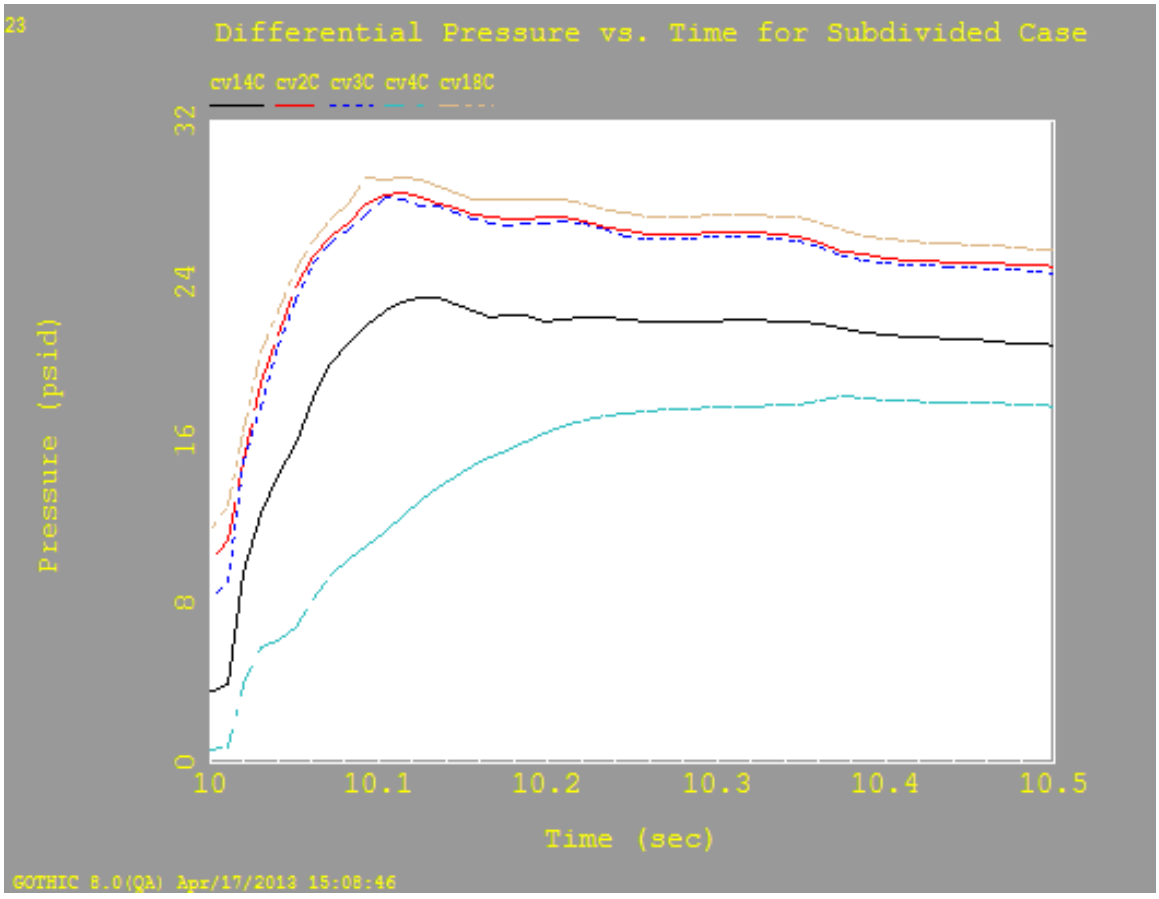

Figure 20: Differential Pressure vs. Time for Subdivided case, showing Nodes 2-4, 1s2 (average non-break node), and 1s8 (pipe break node). 1s2 is shown as cv14C, 1s8 is shown as cv18C, and nodes 2-4 are shown as cv#C as in other figures.

It can be seen in Figure 20 that the pressures in nodes 2 to 4 increase slightly to accommodate the distributed average pressure in node 1. However, if these nodes were also subdivided, some decrease in pressure may be seen.

The results of this case are best summarized by Figure 21, which shows the representative high, low, and average curves for the non-break nodes, as well as the pressure in the sub-node that contained the hot leg pipe break.

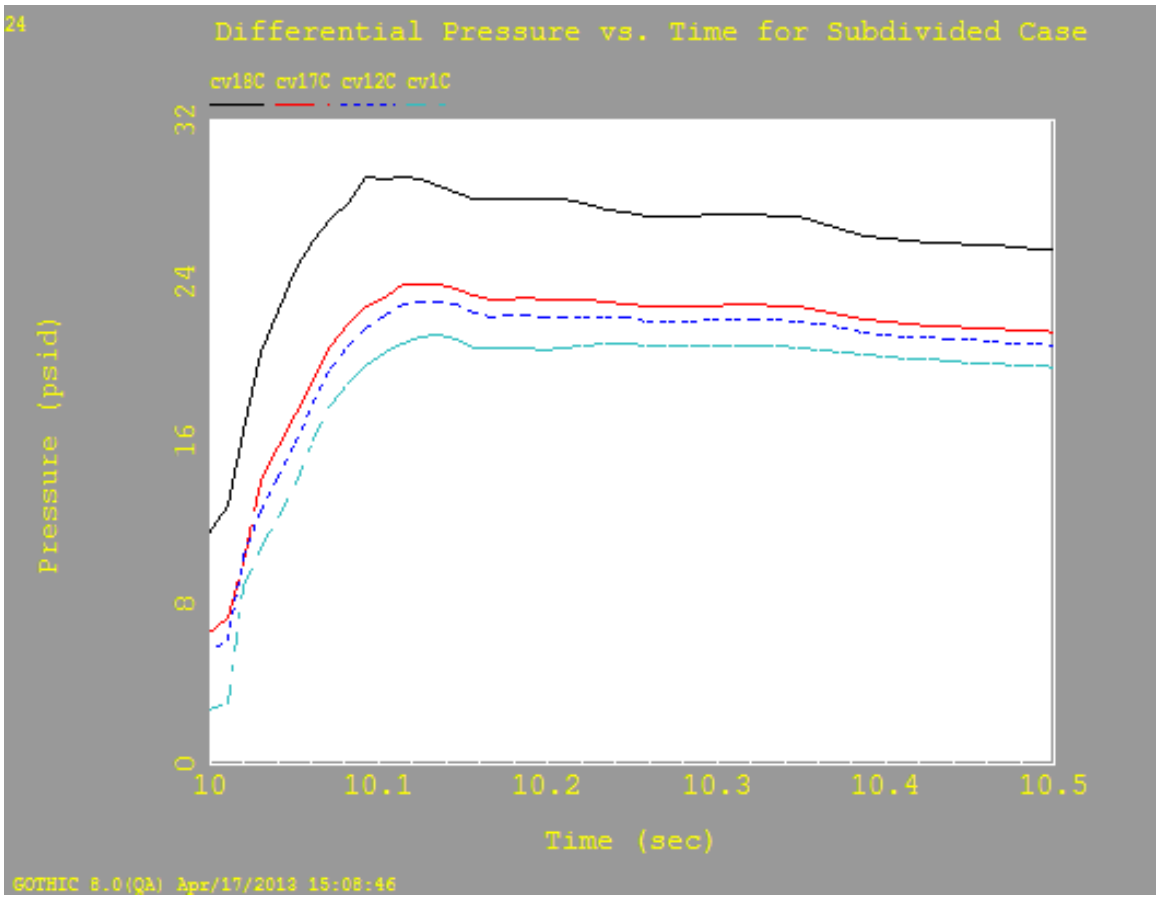

Figure 21: Differential Pressure vs. Time for Subdivided Case, showing representative sub-nodal pressures. cv18C (sub-node 1s8) contains the hot leg pipe break, cv17C (sub-node 1s7) has the highest pressure of the non-break containing nodes, cv1C (sub-node 1s5) has the lowest pressure of the non-break nodes, and cv12C (sub-node 1s4) is nearest to the average value of the non-break nodes.

The node containing the break is about 6.13 psid higher than the pressure of the average non-break node, which represents nearly a 23.45% difference. Additionally, when compared to the base GOTHIC model's results shown in Figure 10, the average peak pressure (in non-break nodes) for the subdivided case is 23.08 psid, while originally it was 27.01 psid. This 3.93 psid decrease constitutes about 15.69% difference in pressure.

For the purpose of applying the results of this analysis, the limitation of the pressure effects on walls is key. Recall that the hot leg pipe rupture is assumed to be central to the side of the node. If the break could be more definitively located, the difference in the local pressure near the pipe break and the rest of the node could be utilized. A lower local pressure next to a wall (which is the limiting factor) creates the design margin desired. However, the pressure release in a hot leg pipe would be due to an unexpected pipe break (due to fatigued or faulty welds or materials) and may not be easily isolated.

Some potential ways that the hypothetical pipe break could be located are by reinforcing all but one section of pipe, or by placing blast shields to control pressure gradients near pressure-sensitive components. Each of these carries its own benefit and cost.

Reinforcing pipes could potentially benefit by leaving all sections of pipe stronger than selected isolated sections, thus ensuring that if there is a failure, it will likely happen in the weakest section. However, if doing this, why not simply reinforce the entire pipe, creating an overdesign that would remain safe at significantly greater cost? Additionally, the reinforcing material could actually create additional stress on the pipes during thermal expansion/contraction and mechanical vibration which may cause a rupture rather than prevent it. This option would need to be weighed and executed well to ensure that there are no unintended consequences.

The idea of placing blast shields near pressure sensitive equipment and walls seems a more feasible one. Part of the pressure increase in the distribution shown in Figure 19 around the pipe break is indicative of the momentum of the steam release before it has a chance to diffuse to surrounding nodes. As long as that momentum is unable to reach a pressure sensitive wall, the local pressure in that node will remain lower. Thus, a pipe break with closer proximity to a wall that is directed away would have little additional effect on the pressure seen by the wall. Care would need to be taken in securing any blast shields placed in containment, however, to prevent them from becoming missile hazards, which could cause more damage than they avert.

Regardless of how the pipe break is localized, the increased nodalization of the model provides important information. That information is necessary to design for the higher pressures near the break, while utilizing the lower pressures in the surrounding sub-nodes. With the areas away from the break being over 23% lower than that near the break, and those areas also being over 15% lower than the original model, it is possible to utilize these differences to create some desired design margin.

5 Conclusions and Recommendations

The lumped parameter model created in GOTHIC simulated the effects of a loss of coolant accident in a steam generator subcompartment of the containment structure for a reactor at the North Anna Power Station. Once a lumped parameter approach using the GOTHIC software was justified, it was important to understand the complexities in modeling critical flow phenomena, as critical flow greatly affected the model.

Understanding the UFSAR containment model was the next hurdle, so that a GOTHIC model could be created that would allow for comparison between the two methods. With the basis for comparison established, any results obtained by GOTHIC could be assumed to be valid for the existing containment model. Differential pressure between the steam generator subcompartment and bulk containment was the primary metric for measuring and comparing the results of each model.

The GOTHIC base model that was created was found to match the UFSAR model within acceptable limits. A goal for this study was to analyze the effects of nodalization on the results of the model. Since node 1 had the highest pressures, and node 2 had the next highest, and further since the maximum pressure was the factor of interest, nodes 1 and 2 were the focus of modifications within the model.

The first nodalization experiment that was performed was to combine nodes 1 and 2 to check the effects of decreasing the number of nodes in the model. As predicted, there was a very slight, though nearly negligible decrease in differential pressures as compared to the base model.

The second, and more telling nodalization experiment was examining the effects of increasing nodalization. Node 1 was the subject of this experiment, and it was subdivided into 9 sub-nodes. The increased detail offered in this experiment showed that, while there was a local increase in pressure around the pipe break, that pressure quickly dissipated and the sub-nodes in the rest of node 1 showed over 15% lower pressures as compared to the base model.

The drastic reduction in pressures away from the pipe break, if applied correctly, could present desired design margin. With this knowledge, further study in a couple directions may be warranted.

First, it may be valuable to take the analysis contained herein further. Attempting to answer the question 'what level of detail is necessary and beneficial in this type of analysis?' will determine what, if any, extra value may be obtained by additional subnodalization. Any application of this analysis or expansion of this analysis will still have to deal with the situation created by the local spike in pressure around the pipe break, and modeling its dispersal and effects when placed next to a wall. Additionally, while GOTHIC has been benchmarked in large scale applications, further study into how GOTHIC approaches multiple smaller compartments and nodalization schemes may be valuable to improving the analysis.

Second, some value could be found in reorganizing the nodalization scheme. By examining how not just the number of nodes, but how their placement affects model results, a better approximation of the system may be obtained. Additionally, since a pipe may break in any location, it is necessary to perform multiple model runs that address the location of the pipe break. The reason that the UFSAR model originally split the pipe break between two nodes is

not explicitly stated, but it may be beneficial when reorganizing the nodes to place the entire pipe break within a single node.

Ultimately, nodalization has proven to have an effect on the overall model accuracy and usefulness. While combining nodes did not present any significant results, the subdivision of node 1 affected the pressures throughout that node and the entire model. More subdivided nodes and a greater refinement in the subdivisions and overall nodalization may be able to refine the model to the point of demonstrating justifiable design margin. Additional experimentation would be beneficial in attempting to ascertain exactly how this information could be utilized to improve models of a typical PWR, such as those at the North Anna Power Station, under these conditions.

6. References

1. *North Anna Power Station Updated Final Safety Analysis Report*, Dominion Power. Chapter 6.

2. Commission, U.S.N.R. *Glossary*. [cited 2013; Available from: http://www.nrc.gov/reading-rm/basic-ref/glossary.html.

3. Karwat, H., *Containments — Design principles and background.* Nuclear Engineering and Design, 1985. **90**(2): p. 113-133.

4. Norris, W.E., D.J. Naus, and H.L. Graves Iii, *Inspection of nuclear power plant containment structures.* Nuclear Engineering and Design, 1999. **192**(2–3): p. 303-329.

5. Shockling, M.A., C. Frepoli, and K. Ohkawa, *Safety - Simulation - Calculating LOCA system effects*, in *Nuclear Engineering International,* 2012, Wilmington Publishing Limited. p. 24.

6. Bermúdez, A. and F. Pena, *Galerkin lumped parameter methods for transient problems.* International Journal for Numerical Methods in Engineering, 2011. **87**(10): p. 943-961.

7. Povilaitis, M., E. Urbonavičius, and S. Rimkevičius, *Modeling of atmosphere stratification in containments of nuclear power plants using lumped-parameter code.* Nuclear Engineering and Design, 2011. **241**(8): p. 3111-3120.

8. Munson, B.R., D.F. Young, and T.H. Okiishi, *Fundamentals of fluid mechanics,* 2006, Hoboken, NJ: J. Wiley & Sons.

9. Installations, O.N.E.A.C.o.t.S.o.N., *Critical flow modelling in nuclear safety : a state-of-the-art report,* 1982, Paris, France; Washington, D.C.: Nuclear Energy Agency, Organisation for Economic Co-operation and Development ; OECD publications and Information Center.

10. Sokolowski, L. and T. Kozlowski, *Assessment of Two-Phase Critical Flow Models Performance in RELAP5 and TRACE Against Marviken Critical Flow Tests*, 2012, Nuclear Regulatory Commission.

11. Johnson, R.W., *The handbook of fluid dynamics,* 1998, Boca Raton, Fla.: CRC Press.

12. Moody, F.J., *Maximum Two-Phase Vessel Blowdown From Pipes*, 1965, General Electric: San Jose, California.

13. D'Auria, F. and P. Vigni, *Two-Phase Critical Flow Models*, 1980, Nuclear Energy Agency.

14. Fauske, H.K., *Contribution to the Theory of Two-Phase, One-Component Critical Flow*, 1962, Argonne National Laboratory: Argonne, Illinois.

15. Todreas, N.E. and M.S. Kazimi, *Nuclear systems. Vol. 1, Thermal hydraulic fundamentals,* 2012, Boca Raton: CRC Press : Taylor & Francis.

16. Ardron, K.H.a.F., R.A., *A study of the Critical Flow Models Used In Reactor Blowdown Analysis.* Nuclear Engineering and Design, 1976. **39**(2-3): p. 257-266.

17. Zaloudek, F.R., *Steam-Water Critical Flow From High Pressure Systems Interim Report*, 1964, Hanford Laboratories: Richland, Washington.

18. Knee, D., *Critical Flow Model*, 2012, E-mail conversation.

19. Starkman, E.S., et al., *Expansion of a Very Low Quality Two-Phase Fluid Through a Convergent-Divergent Nozzle.* Journal of Basic Engineering, 1964. **86**(2).

20. Richter, H.J., *Separated two-phase flow model: application to critical two-phase flow.* International Journal of Multiphase Flow, 1983. **9**(5): p. 511-530.

21. Trapp, J.A. and V.H. Ransom, *A choked-flow calculation criterion for nonhomogeneous, nonequilibrium, two-phase flows.* International Journal of Multiphase Flow, 1982. **8**(6): p. 669-681.

22. Wiles, L.E. and T.L. George, *Thermal-hydraulic analysis of the nuclear power engineering corporation containment experiments with GOTHIC.* Nuclear technology, 2003. **142**(1): p. 77-91.

23. *GOTHIC Thermal Hydraulics Analysis Package Qualification Report*, 2012.

24. Chen, Y.-S., et al., *Pressure and temperature analyses using GOTHIC for Mark I containment of the Chinshan Nuclear Power Plant.* Nuclear Engineering and Design, 2011. **241**(5): p. 1548-1558.

25. Chen, Y.-S., Y.-R. Yuann, and L.-C. Dai, *Lungmen ABWR containment analyses during short-term main steam line break LOCA using GOTHIC.* Nuclear Engineering and Design, 2012. **247**(0): p. 106-115.

26. Knee, D. and A. Gharakhanian, *GOTHIC Methodology for Analyzing the Response to Postulated Pipe Ruptures Inside Containment*, 2006, Dominion Power.

27. Wolf, L., H. Holzbauer, and M. Schall, *Comparisons between multidimensional and lumped-parameter GOTHIC containment*

analyses with data. Nuclear technology, 1999. **125**(2): p. 155-165.

28. *GOTHIC Thermal Hydraulic Analysis Package User Manual*, 2012.

29. *GOTHIC Thermal Hydraulic Analysis Package Technical Manual*, 2012.

30. George, T.L. and A. Singh, *Separate effects tests for gothic condensation and evaporative heat transfer models.* Nuclear Engineering and Design, 1996. **166**(3): p. 403-411.

31. *Application for Renewed Operating Licenses - North Anna Power Station Units 1 and 2*, Dominion Power: www.nrc.gov.

32. Jeon, S.-J. and C.-H. Chung, *Axisymmetric modeling of prestressing tendons in nuclear containment dome.* Nuclear Engineering and Design, 2005. **235**(23): p. 2463-2476.

33. *North Anna Power Station Updated Final Safety Analysis Report*, Dominion Power. Chapter 3.

34. *Introductory GOTHIC Training Course*, 2012, Numerical Applications, Inc.: Richland, WA.

Appendix A: GOTHIC Input Parameters

Table 5: Volume Parameters

Node #	Volume (ft^3)	Elevation (ft)	Height (ft)	Hydraulic Diameter (ft)	L/V Interface Area (ft^2)
1	3080	243	16	13.8744	Default
2	3670	243	16	15.1451	Default
3	1960	243	16	11.068	Default
4	5780	243	16	19.0066	Default
5	2730	259	3.5	27.9285	Default
6	6970	262.5	9	27.8288	Default
7	11650	271.5	16	26.9828	Default
8	2825	291.833	10	16.8077	Default
9	1340	236.667	6.3333	14.5458	Default
10	1590297	0	400	63.0537	Default

Table 6: Boundary Condition Parameters

BC#	Pressure (psia)	Temp (F)	Flow (lbm/s)	Liquid Volume Fraction	Steam Volume Fraction	Drop Diameter (in)
1F	Forcing Function	Enthalpy Table	Forcing Table	1	1	0.0039
2F	Forcing Function	Enthalpy Table	Forcing Table	1	1	0.0039

Table 7: Run Control Parameters

Time Dom	DT Min	DT Max	DT Ratio	End Time	Print Int	Graph Int
1	1.00E-06	0.01	1	10	0.1	0.1
2	1.00E-06	0.01	1	11.5	0.1	0.01

Table 8: Flow Path Parameters

Flow Path #	Between Nodes	Vent Area (ft^2)	Hydraulic Dia. (ft)	Inertia Length (ft)	Friction Length (ft)	Roughness (dim)	Flow Loss Coeff.	Exit Loss Coeff.
1	1-9	66.1	9.1739	5	1	0.1	0.5	0.53
2	2-9	68.9	9.3662	5	1	0.1	0.65	0.51
3	3-9	45	7.5694	5	1	0.1	0.62	0.66
4	1-5	56	8.444	5	1	0.1	0.36	0.86
5	2-5	119	12.3092	5	1	0.1	0.2	0.72
6	3-5	72	9.5746	5	1	0.1	0.21	0.82
7	4-5	237	17.3712	5	1	0.1	0.02	0.48
8	5-6	690	29.6401	5	1	0.1	0.33	0
9	6-7	565	26.8213	5	1	0.1	0.13	0.05
10	7-8	140	13.3512	5	1	0.1	0.47	0.34
11	9-10	64	9.027	20	5	0.1	0.5	1
12	9-10 B	93	10.8817	20	5	0.1	0.38	1
13	4-10 B	21.4	5.2199	20	5	0.1	0.83	1
14	6-10 B	21.4	5.2199	20	5	0.1	0.83	1
15	7-10	202.3	16.0492	20	5	0.1	0.5	1
16	8-10	256.2	18.0611	20	5	0.1	0.1	1
17	1F-1	2.2935	1.7089	5	1	0.1	0	0
18	2F-2	2.2935	1.7089	5	1	0.1	0	0
19	1-2	189	15.5126	5	1	0.1	0.1	0.18
20	1-4	24	5.5279	5	1	0.1	0.47	0.47
21	2-3	258	18.1245	5	1	0.1	0.1	0.05
22	2-4	24	5.5279	5	1	0.1	0.48	0.91
23	3-4	24	5.5279	5	1	0.1	0.45	0.91

Table 9: Valve Parameters

Valve #	Flow Path #	Open Trip #	Valve Type #	Discharge Volume
1V	12	1	1	10
2V	13	2	2	10
3V	14	3	2	10

Valve Type

Valve Type #	Valve Option	Full Open Cd
1	Q Open	1
2	Q Open	1

Table 10: Trip Parameters

Component Trips

Trip #	Sense Var.	Sensor 1 Loc.	Var Limit	Set Point	Delay Time	Cond Type
1	CONT	9C	UPPER	5	0	AND
2	CONT	4C	UPPER	5	0	AND
3	CONT	6C	UPPER	5	0	AND
4	TIME		UPPER	0	0	AND

Table 11: Initial Condition Parameters

Vol #	Total Pressure (psia)	Vapor Temp (F)	Liquid Temp (F)	Relative Humidity (%)	Liquid Volume Fract.
def	8.6	120	32	0	0
1	8.6	120	32	0	0
2	8.6	120	32	0	0
3	8.6	120	32	0	0
4	8.6	120	32	0	0
5	8.6	120	32	0	0
6	8.6	120	32	0	0
7	8.6	120	32	0	0
8	8.6	120	32	0	0
9	8.6	120	32	0	0
10	8.6	120	32	0	0

Appendix B: Mass and Energy Release Data

Table 12: Mass and Energy Release Rates for Hot Leg Single Ended Split. Data provided to Dominion Power by Westinghouse. Copyright Dominion Power; Used with permission.

Table 6.2-9
SATAN V MASS AND ENERGY RELEASE RATES
HOT LEG SINGLE-ENDED SPLIT

Time (sec)	Mass Flow Rate (10^3 lbm/sec)	Energy Flow Rate (10^6 Btu/sec)
0.0	0.0	0.0
0.001	3.540	23.20
0.002	4.354	28.48
0.0060	3.696	23.94
0.0130	4.187	27.03
0.0170	4.178	26.96
0.0260	4.313	27.83
0.381	4.523	29.22
0.0440	4.611	29.82
0.0450	4.966	32.15
0.0470	4.698	30.38
0.0510	4.778	30.90
0.0540	4.781	30.93
0.0600	4.697	30.43
0.0700	4.618	30.03
0.0780	4.582	29.95
0.0840	4.618	30.27
0.0919	4.798	31.48
0.1000	4.606	30.19
0.1500	4.274	28.24
0.2001	4.342	28.49
0.2500	4.194	27.48
0.3002	4.234	27.70
0.3401	4.189	27.40
0.3701	4.205	27.50
0.4500	4.183	27.31
0.5002	4.140	27.07
0.6001	3.939	26.07
0.6703	3.861	25.56
0.7802	3.904	25.41
0.8501	3.865	25.21
0.8802	3.825	25.05
0.9501	3.729	24.62
1.0001	3.672	24.29
1.5002	3.222	21.53

*Note that there is a mistake in the table, the Mass Flow Rate exponent should be 10^4 lbm/sec.